

# SORET DRIVEN DOUBLE DIFFUSIVE RAYLEIGH BENARD MARANGONI CONVECTION IN A COMPOSITE LAYER SUBJECTED TO UNIFORM AND NON UNIFORM SALINITY GRADIENTS WITH INTERNAL HEAT SOURCE

<sup>1</sup>Veeranna. Y., <sup>2</sup>Shivaraja. J. M., <sup>3</sup>T. Arul Selvamary., <sup>4</sup>Sumithra. R., <sup>5</sup>Sumithra N,  
<sup>6</sup>Thejas Yadav D.

<sup>1&4</sup>Associate professor and professor, Department of UG, PG Studies & Research in Mathematics, Government Science College (Autonomous), Nrupathunga University, Nrupathunga Road, Bengaluru – 560 001, Karnataka.

<sup>2</sup>Assistant professor, Department of Mathematics, Bengaluru North University, Tamaka, Kolar.

<sup>3</sup>Assistant professor, Department of Mathematics, Jyothi Nivasa College Autonomous affiliated to Bengaluru City University, Bengaluru, Karnataka.

<sup>5</sup>Sumithra N and <sup>6</sup>Thejas Yadav D, Pg students, Government Science College (Autonomous), Nrupathunga University, Nrupathunga Road, Bengaluru– 560 001, Karnataka.

**Abstract :** The stability analysis of Soret-driven double-diffusive Rayleigh–Bénard–Marangoni convection in a composite system subjected to uniform and non-uniform salinity gradients with an internal heat source is investigated theoretically. The system is bounded by a lower rigid surface and an upper free horizontal surface, both of which are adiabatically insulated to temperature and concentration. The system is exposed to both uniform and non-uniform salinity gradients. A two-layer model is employed to describe the momentum equations for the fluid and porous layers, governed by the Navier-Stokes and Darcy equations, respectively. Graphs are plotted using MATHEMATICA to examine the effects of various dimensionless parameters, including the solute Rayleigh number, Soret number, Darcy number, thermal diffusivity ratio, thermal Marangoni number, solute Marangoni number, internal Rayleigh number, thermal depth, solute diffusivity ratio, and the ratio of solute to thermal diffusivity, on the onset of double-diffusive Rayleigh–Bénard–Marangoni convection. The analysis reveals that the solute Rayleigh number, Soret number, solute diffusivity ratio, and the ratio of solute to thermal diffusivity exert a stabilizing influence on the convection onset. In contrast, the Darcy number and thermal diffusivity ratio have a destabilizing effect, regardless of the type of salinity gradient applied.

**Key words:** Double Diffusive Rayleigh - Benard Marangoni Convection, Soret Effect, Salinity Gradients, Internal Heat Source.

## 1. Introduction

Marangoni convection refers to fluid motion driven by surface tension gradients. Even small variations in temperature or solute concentration can generate significant convection, as surface tension on a free surface is highly sensitive to these parameters. The thermal diffusion process, commonly referred to as the Soret effect, arises due to a salinity gradient. A horizontal composite layer system comprising porous and fluid layers, with heat and mass transfer occurring across the interface, is relevant to numerous natural phenomena and industrial applications. A related scenario involving a liquid layer above a porous layer is frequently encountered in environmental and engineering contexts. Examples include the water layer of a pond or lake with a muddy bottom, transport processes between soil and water, and geothermal systems. The Soret effect, or thermodiffusion, represents the mass flux within a mixture induced by a temperature gradient. Although this effect is typically weak, it plays a significant role in the analysis of compositional variations in hydrocarbon reservoirs and similar systems. Nield and Bejan (1992) devoted a collection of their works in the area of convection in porous media in their book. They defined a porous medium as a material consisting of a solid matrix with an interconnected void. The solid matrix is either rigid or undergoes small deformations. The interconnectedness of the void (the pores) allows the flow of one or more fluids through the material. Kim et al (1996) the onset of convection when a porous layer underlying a fluid layer is heated from below has been numerically investigated. In order to validate the interface boundary conditions along with the numerical scheme, the present study has focused on the critical Rayleigh number and the corresponding number of cells. The results show that the number of cells at the critical Rayleigh number is in good agreement with the previous report based on the linear stability theory. Bergeon et al (1998) investigated numerically the Marangoni convection with Soret effect in a binary mixture. M. Z. Saghir (1998) numerically investigates the interaction between the Marangoni and the double diffusive convection. The model consists of a two-cavity rectangular system in which the smaller cavity is located at the top left corner of the larger one. Finite element modelling results indicate that salinity induces stronger convection than the thermal ones. D. Schwabe (1999) the multi-roll-structure with convection rolls, all with the same sense of rotation and axes perpendicular to the applied temperature gradient appears in thin layers driven by thermocapillarity prior to time dependent states. Detailed experimental and numerical results are reported. D. Schwabe (1999) Bénard-Marangoni-Instability is studied due to surface tension forces in the free oil surface. The layer was partly covered with a solid lid from Polycarbonate at the end of the microgravity time an instability of the boundary between two convection cells in the container is found. Josef Tanny et al (1999) investigate the mixing process of a two-layer stratified fluid in a laterally heated

en- closure. Due to the lateral heating of the enclosure, a circulating flow is induced in each layer such that the interface separating the layers is simultaneously exposed to destabilizing shear and double diffusive convection. The results show that when the flow adjacent to the interface is unstable, it is characterized by intense vortices and the mixing time is relatively short. Bahloul et al (2003) the Marangoni flows in a horizontal layer of a binary mixture with an undeformable free upper surface are studied analytically and numerically. The system is heated and cooled by constant heat fluxes. The validity of the analytical model is tested against the results obtained by solving numerically the full governing equations. C.G. Jiang et al (2004) investigate the convection effect in a vertical cavity subject to a lateral heating condition based on two-dimensional numerical simulation.. The thermal diffusion process is simulated in a vertical porous media combined with natural convection flow. Numerical results reveal that the lighter fluid component migrates to the hot side of the cavity, and as the permeability increases, the component separation in the thermal diffusion, or Soret effect, process increases first, reaches its peak, and then decreases. Adrian Postelnicu (2004) studied simultaneous heat and mass transfer by natural convection from a vertical flat plate embedded in electrically conducting fluid saturated porous medium, using Darcy–Boussinesq model, including Soret and Dufour effects. The effects of the governing parameters on the heat and mass transfer are studied. Kozak and Saghir(2004) studied Marangoni convection in a liquid layer overlying a porous layer taking into consideration evaporation at the free surface. They studied different aspect ratios, thickness ratios and temperatures for the pure thermocapillary case. For lateral heating case, they found that switching of the flow from the liquid layer into the porous layer is due to the ratio of liquid thickness to the porous thickness. M.Z Saghir and P.Mahendran (2005) studied Marangoni and gravity driven convection in a liquid layer overlying a porous layer. They analyzed the onset of thermal convection for both the bottom and lateral heating conditions. For the bottom heating case, they found that when natural convection was in the liquid layer, the aspect ratio changed the flow configuration. However, when the natural convection was in the porous layer, the aspect ratio had no effect on the flow pattern. They also found that large convective motion was present for a low thickness ratio and weakens as the thickness ratio increased further. For both bottom and lateral heating cases, they found that the liquid layer thickness determines whether the flow is dominant in the liquid layer or in the porous layer and in some cases multi-cell formation occurs due to changing of the aspect ratio. A comprehensive review of the natural convection due to combined thermal and solutal driving forces was conducted by Nield and Bejan (1999), Ingham and Pop (2005). A system containing two or more components whose concentrations vary from point to point,

in such a system, there is a natural tendency for mass to be transferred, minimizing the concentration differences within the system and the transport of one constituent, from a region of higher concentration to that of a lower concentration. This is called mass transfer. Li Mingchun et al (2006) studied thermal-diffusion (Soret) and the diffusion-thermo (Dufour) effects. The properties of the heat and mass transfers in a strongly endothermic chemical reaction system for a porous medium are numerically studied. Through the theory of the thermodynamics of irreversible processes, a coupled mathematical model describing the heat and mass transfers in a porous system for the calcination of limestone is formulated. The results indicate that when the convective velocity is lower or when the initial temperature of the feeding gas is higher, Soret and Dufour effects can't be ignored. I.S.Shivakumara et al (2006) investigated the onset of surface-tension-driven convection is studied in a two-layer system comprising an incompressible fluid-saturated porous layer over which lies a layer of the same fluid. The lower rigid surface of the porous layer is either perfectly heat conducting or insulating, while the upper heat insulating fluid boundary is free and at which the surface tension effects are allowed for. The effect of variation of different physical parameters on the onset of Marangoni convection is investigated in detail. Mansour et al(2008) studied the thermosolutal convection developed in a horizontal shallow porous layer salted from below and subject to a cross flux of heat. They studied the combined effect of thermodiffusion and lateral heating on double diffusive natural convection in a horizontal porous layer, filled with a binary fluid and subjected to uniform fluxes of heat and mass on its long sides. Benoit Trouette et al (2012) Solutal driven flow is studied for a binary solution submitted to solvent evaporation at the upper free surface This problem is studied numerically, using several assumptions deduced from previous experiments on polymer solutions. The stability of the system is investigated as a function of the solutal Rayleigh and Marangoni numbers, the evaporative flux and the Schmidt number. Sumithra et al(2020) investigated analytically the effect of Soret parameter on double diffusive Marangoni convection in a two-layer system, comprising an incompressible two component fluid saturated porous layer over which lies a layer of the same fluid under micro gravity condition. Sumithra et al(2020) have considered a composite system to analyze the effect of the Soret parameter on the double-diffusive Marangoni convection using the exact method. They have concluded that with the increase in the Soret coefficient, the system develops instability. Sumithra et al(2021) studied the effect of thermal diffusion on the onset of double-diffusive convection in a composite system. The porous layer of the composite system is modeled employing the Darcy–Brinkman–Rayleigh–Benard model. The boundaries of the composite system are assumed to be rigid-rigid under

normal gravitational force. Khalid et al (2022) Rayleigh-Benard convection in rotating nanofluids layer with feedback control and double-diffusive coefficients heated from below is examined. The system is considered for three types of lower-upper boundary conditions, free-free, rigid-free and rigid-rigid. Based on the observation, the effect of increasing the value of rotation, feedback control, Dufour parameter and solutal Rayleigh number are observed to stabilize the system. Meanwhile, the effect of increasing the value of Soret parameter, nanofluids Lewis number, nanoparticles concentration Rayleigh number and modified diffusivity ratio are found to destabilize the system. Sumithra et al(2022) investigated the physical configuration of the problem of Darcy Brinkman Rayleigh Benard Convection in a two-layered system has been investigated for linear, parabolic and inverted parabolic salinity gradients with the Dufour effect. The regular perturbation methodology has been used to solve the governing equations of the composite system with the Boussinesq approximation. Sumithra et al(2023) investigated composite system possessing rigid-rigid boundaries, the significance of thermal diffusion on the onset of triple diffusive convection is analyzed. The Darcy–Brinkman–Rayleigh–Benard model is employed to model the porous media. The present investigation is to study the effect of uniform and non-uniform salinity gradients on the onset of double-diffusive convection in composite layer under the influence of Soret effect and internal heat source.

## 2. Mathematical Formulation

**Mathematical formulation** We consider a homogeneous porous layer of thickness  $d_m$  underlying an incompressible liquid layer of thickness  $d$ . Cartesian coordinates are used with origin at the liquid - porous interface. The  $z$  direction is opposite to the gravitational acceleration  $\vec{g}$ . The bottom of the porous layer is a rigid, and the upper surface of the fluid is free and the system is adiabatically insulated for heat and mass. The temperature difference of fluid layer is  $T_0 - T_u$  and of the porous layer is  $T_l - T_0$  and that of the total system is  $T_l - T_u$ . The concentration difference of fluid layer is  $C_0 - C_u$ , of the porous layer is  $C_l - C_0$ . And that of the total system is  $C_l - C_u$ .

### Governing Equations

Under the Boussinesq approximation, the equation of continuity, the equation of fluid, the heat equation and the concentration equation and the equation of state are given by

**For fluid layer,**

Equation of Continuity,

$$\nabla_{f1} \cdot \vec{q}_{f1} = 0 \quad (1)$$

Equation of Momentum,

$$\rho_0 \left[ \frac{\partial \vec{q}_{f1}}{\partial t} + (\vec{q}_{f1} \cdot \nabla_{f1}) \vec{q}_{f1} \right] = -\nabla_{f1} P_{f1} + \mu \nabla_{f1}^2 \vec{q}_{f1} - \rho_{f1} g \hat{k} \quad (2)$$

Equation of Energy,

$$\frac{\partial T_{f1}}{\partial t} + (\vec{q}_{f1} \cdot \nabla_{f1}) T_{f1} = k_{T_{f1}} \nabla_{f1}^2 T_{f1} + Q_{f1} \quad (3)$$

Equation of Concentration,

$$\frac{\partial \vec{C}_{f1}}{\partial t} + (\vec{q}_{f1} \cdot \nabla_{f1}) \vec{C}_{f1} = k_{\vec{C}_{f1}} \nabla_{f1}^2 \vec{C}_{f1} + k_{T_{f1}} \nabla_{f1}^2 T_{f1} \quad (4)$$

Equation of State,

$$\rho_{f1} = \rho_0 \left( 1 - \alpha_{T_{f1}} (T_u - T_0) + \alpha_{\vec{C}_{f1}} (C_u - C_0) \right) \quad (5)$$

**For porous layer,**

Equation of Continuity,

$$\nabla_{m1} \cdot \vec{q}_{m1} = 0 \quad (6)$$

Equation of Momentum,

$$\rho_0 \left[ \frac{1}{\varphi} \frac{\partial \vec{q}_{m1}}{\partial t} + \frac{1}{\varphi^2} (\vec{q}_{m1} \cdot \nabla_{m1}) \vec{q}_{m1} \right] = -\nabla_{m1} P_{m1} - \frac{\mu}{k} \vec{q}_{m1} - \rho_{m1} g \hat{k} \quad (7)$$

Equation of Energy,

$$\varphi \frac{\partial T_{m1}}{\partial t} + (\vec{q}_{m1} \cdot \nabla_{m1}) T_{m1} = k_{T_{m1}} \nabla_{m1}^2 T_{m1} + Q_{m1} \quad (8)$$

Equation of concentration,

$$\varphi \frac{\partial C_{m1}}{\partial t} + (\vec{q}_{m1} \cdot \nabla_{m1}) C_{m1} = k_{C_{m1}} \nabla_{m1}^2 C_{m1} + k_{T_{m1}} \nabla_{m1}^2 T_{m1} \quad (9)$$

Equation of State,

$$\rho_{m1} = \rho_0 \left( 1 - \alpha_{m1} (T_l - T_0) + \alpha_{m1} (C_l - C_0) \right) \quad (10)$$

**Basic state solution**

The basic state solution of the composite system is obtained for the quiescent flow where velocity, temperature, concentration and pressure are functions of z only and is given by,

For fluid layers,

$$\vec{q}_{f1} = 0, \quad P_{f1} = P_0(z), \quad T_{f1} = T_0(z), \quad \rho = \rho_b(z), \quad C_{f1} = C_{f1b}(z) \quad (11)$$

For porous layers,

$$\left\{ \begin{array}{l} \vec{q}_{m1} = 0, \quad P_{m1} = P_{m1b}(z_{m1}), \quad T_{m1} = T_{m1b}(z_{m1}), \quad \rho_{m1} = \rho_{m1b}(z_{m1}) \\ C_{m1} = C_{m1b}(z_{m1}) \end{array} \right\} \quad (12)$$

The temperatures distributions  $T_b(z)$  and  $T_{m1b}(z_{m1})$  are

$$T_{f1b}(z) = -Q \frac{(z^2 - dz)}{2k_{T_{f1}}} + \left( \frac{(T_u - T_0)}{d} \right) z + T_0 \quad (13)$$

$$T_{m1b}(z_{m1}) = \frac{Q_{m1}}{2k_{T_{m1}}} [z_{m1}^2 + d_{m1}z_{m1}] + \left( \frac{(T_0 - T_1)}{d_{m1}} \right) z_{m1} + T_0 \quad (14)$$

The concentration distributions  $C_b(z)$  and  $C_{m1b}(z_{m1})$  are

$$C_b(z) = C_0 + \frac{(C_u - C_0)z}{d} \quad (15)$$

$$C_{m1b}(z_{m1}) = C_0 + \frac{(C_0 - C_l)z_{m1}}{d_{m1}} \quad (16)$$

At interface temperature ( $T_0$ )

$$T_0 = \left( \frac{T_u k_{T_{f1}} d_{m1} + T_l k_{T_{m1}} d}{d d_{m1}} \right) + \left( \frac{d d_{m1} (Qd + Q_{m1} d_{m1})}{2 (d k_{T_{m1}} + k_{T_{f1}} d_{m1})} \right)$$

At interface concentration ( $C_0$ )

$$C_0 = \frac{C_u k_{C_{f1}} d_{m1} + C_l k_{C_{m1}} d}{k_{C_{m1}} d + k_{C_{f1}} d_{m1}}$$

### 3. Linear Stability Analysis

#### Perturbed state

In order to investigate the stability of the basic solution, we superpose perturbations on the system in the form.

for fluid layers,

$$\vec{q}_{f1} = 0 + \vec{q}'_{f1}, \quad P_{f1} = P_{f1b}(z) + P' \quad (17)$$

$$T_{f1} = T_{f1b}(z) + \theta_{f1}, \quad C_{f1} = C_{f1b}(z) + \phi \quad (18)$$

For porous layers,

$$\vec{q}_{m1} = 0 + \vec{q}'_{m1b}, \quad P_{m1} = P_{m1b}(z_{m1}) + P'_{m1} \quad (19)$$

$$C_{m1} = C_{m1b}(z_{m1}) + \phi_{m1}, \quad T_{m1} = T_{m1b}(z_{m1}) + \theta_{m1} \quad (20)$$

The above equations are substituted in equations (1) to (10) and are linearized in the usual manner. By taking curl twice on equations (2) and (7), the pressure term is eliminated and only the vertical component is retained. The variables are then non-dimensionalized by choosing separate length scales for the two layers so that each layer is of unit depth. Thus we obtained non-dimensional linearized equations for momentum, temperature, concentration in fluid and porous layers respectively.

for fluid layers,

$$\left\{ \begin{array}{l} (u, v, w) = \frac{k_T}{d} (u^*, v^*, w^*), \quad \theta_{f1} = (T_0 - T_u)\theta_{f1}^*, \quad \nabla_{f1} = \frac{1}{d} \nabla_{f1}^* \\ (x, y, z) = d(x^*, y^*, z^*), \quad \phi_{f1} = (C_0 - C_u)\phi_{f1}^*, \quad t_{f1} = \frac{d^2}{k_{Tf1}} t_{f1}^* \end{array} \right\} \quad (21)$$

For porous layers,

$$\left\{ \begin{array}{l} (u_{m1}, v_{m1}, w_{m1}) = \frac{k_{Tm1}}{d_{m1}} (u_{m1}^*, v_{m1}^*, w_{m1}^*), \quad \theta_{m1} = (T_l - T_0)\theta_{m1}^*, \quad \nabla_{m1} = \frac{1}{d_{m1}} \nabla_{m1}^* \\ (x_{m1}, y_{m1}, z_{m1}) = d_{m1}(x_{m1}^*, y_{m1}^*, z_{m1}^*), \quad \phi_{m1} = (C_l - C_0)\phi_{m1}^*, \quad t_{m1} = \frac{d_{m1}^2}{k_{Tm1}} t_{m1}^* \end{array} \right\} \quad (22)$$

Substituting (21) and (22) in the above equations for momentum, temperature, concentration in fluid and porous layers. We obtain the following non-dimensionalised equations.

For fluid layer,

$$\frac{1}{Pr_{f1}} \frac{\partial(\nabla_{f1}^2 w)}{\partial t_{f1}} = \nabla_{f1}^4 w + \nabla_{f1}^2 \theta_{f1} Ra_{Tf1} - \nabla_{f1}^2 \phi_{f1} Ra_S \quad (23)$$

$$\frac{\partial \theta_{f1}}{\partial t_{f1}} - w = \nabla_{f1}^2 \theta_{f1} + R_l(2z - 1)w \quad (24)$$

$$\frac{\partial \phi_{f1}}{\partial t_{f1}} - w = \tau \nabla_{f1}^2 \phi_{f1} + S_r \nabla_{f1}^2 \theta_{f1} \quad (25)$$

For porous layer,

$$\frac{Da}{Pr_{m1}} \frac{\partial(\nabla_{m1}^2 w_{m1})}{\partial t} = -\nabla_{m1}^4 w_{m1} + \nabla_{m1}^2 \theta_{m1} Ra_{Tm1} - \nabla_{m1}^2 \phi_{m1} Ra_{Sm1} \quad (26)$$

$$A \frac{\partial \theta_{m1}}{\partial t_{m1}} - w_{m1} = \nabla_{m1}^2 \theta_{m1} + R_{lm1}(2z_{m1} - 1)w_{m1} \quad (27)$$

$$\phi_{m1} \frac{\partial \phi_{m1}}{\partial t_{m1}} - w_{m1} = \tau_{m1} \nabla_{m1}^2 \phi_{m1} + S_{r_{m1}} \nabla_{m1}^2 \theta_{m1} \quad (28)$$

Where,

$Pr_{f1} = \frac{\mu}{\rho_0 k_{Tf1}}$  is the Prandtl number in fluid layer.

$Ra_{Tf1} = \frac{\rho_0 d^3 g \alpha_T (T_0 - T_u)}{\mu k_{Tf1}}$  is Rayleigh number in fluid layer.

$Ra_S = \frac{\rho_0 d^3 g \alpha_C (C_0 - C_u)}{\mu k_{Tf1}}$  is solute Rayleigh number in fluid layer.

$S_r = \frac{\tau(T_0 - T_u)}{(C_0 - C_u)}$  is soret number in fluid layer.

$\tau_{f1} = \frac{k_{Cf1}}{k_{Tf1}}$  is the ratio of solute to temperature diffusivity in fluid layer.

$Pr_{m1} = \frac{\mu\phi_{m1}}{\rho_0 k_{T_{m1}}}$  is the Prandtl number in porous layer.

$Ra_{T_{m1}} = \frac{\rho_0 d g \alpha'_T (T_l - T_0)}{\mu k_{T_{m1}}}$  is Rayleigh number in porous layer.

$Ra_{S_{m1}} = \frac{k \rho_0 d^3 g \alpha_C (C_l - C_0)}{\mu k_{C_{m1}}}$  is solute Rayleigh number in porous layer.

$Da = \frac{k}{d^2 m_1}$  is solute Rayleigh number in porous layer.

$Sr_{m1} = \frac{k_{C_{m1}} (T_l - T_0)}{k_{T_{m1}} (C_l - C_0)}$  is soret number in porous layer.

$\tau_{m1} = \frac{k_{C_{m1}}}{k_{T_{m1}}}$  is the ratio of solute to temperature diffusivity in porous layer.

$Ra_{T_{m1}} = \frac{\alpha_{T_{f1}} \hat{k}_{T_{f1}}^2}{\hat{d}^4} Da Ra_{T_{f1}}$  is the Relation between  $Ra_{T_{f1}}$  and  $Ra_{T_{m1}}$

$Ra_{S_{m1}} = \frac{\alpha_{C_{f1}} \hat{k}_{C_{f1}}^2}{\hat{d}^4} Da Ra_S$  is the Relation between  $Ra_S$  and  $Ra_{S_{m1}}$

Thus the momentum equation in porous layer is transformed in terms of

$Ra_{T_{f1}} - Ra_S$ .

$$\frac{Da}{Pr} \frac{\partial \nabla^2 w_{m1}}{\partial t} = -\nabla^2 w_{m1} + \frac{\alpha_{T_{f1}} \hat{k}_{T_{f1}}^2}{\hat{d}^4} Da (\nabla^2 \theta_{m1}) Ra_{T_{f1}} - \frac{\alpha_{C_{f1}} \hat{k}_{C_{f1}}^2}{\hat{d}^4} Da (\nabla^2 \phi_{m1}) Ra_S$$

The non-dimensionalized equations are subjected to normal mode expansion on the dependent variables in the fluid and porous layers as:

$$\begin{bmatrix} w_{f1} \\ \theta_{f1} \\ \phi_{f1} \end{bmatrix} = \begin{bmatrix} w_{f1}(z) \\ \theta_{f1}(z) \\ \phi_{f1}(z) \end{bmatrix} f(x, y, z) e^{i(lx+my)+nt} \quad (29)$$

$$\begin{bmatrix} w_{m1} \\ \theta_{m1} \\ \phi_{m1} \end{bmatrix} = \begin{bmatrix} w_{m1}(z_{m1}) \\ \theta_{m1}(z_{m1}) \\ \phi_{m1}(z_{m1}) \end{bmatrix} f_{m1}(x_{m1}, y_{m1}, z_{m1}) e^{i(l_{m1}x+m_{m1}y)+n_{m1}t} \quad (30)$$

with  $\nabla^2 f + a^2 f = 0$  and  $\nabla^2_{z_{m1}} f_m + a_{m1}^2 f_{m1} = 0$  where  $a$  and  $a_{m1}$  are the wave numbers,  $n$  and  $n_m$  are the frequencies,  $w$  and  $w_{m1}$  are the dimensionless vertical velocities in the fluid and porous layers respectively. As the principle of exchange of stability is valid for the present problem, the time derivatives are dropped, i.e.,  $n = 0 = n_{m1}$ . Where  $l$  and  $m$  are the horizontal wave number in the  $x$  and  $y$  directions respectively. Substituting equations (29) and (30) in equations (23) to (28), we get the following ordinary differential equations:

for fluid layer,

$$(D_{f1}^2 - a^2)w_{f1}(z) = a^2 (Ra_{T_{f1}}\theta_{f1} - Ra_S\phi_{f1}) \quad (31)$$

$$(D_{f1}^2 - a^2)\theta_{f1}(z) + w_{f1}(z) + (Ra_f(2z - 1)w_{f1}(z) = 0 \quad (32)$$

$$\tau_{f1}(D_{f1}^2 - a^2)\phi_{f1}(z) + w(z) + Sr(D_{f1}^2 - a^2)\theta_{f1}(z) = 0 \quad (33)$$

For porous layer,

$$(D_{m1}^2 - a_{m1}^2)w_{m1}(z_{m1}) = a_{m1}^2(Ra_{Tm1}\theta_{m1} - Ra_{Sm1}\phi_{m1}) \quad (34)$$

$$(D_{m1}^2 - a_{m1}^2)\theta_{m1}(z_{m1}) + w_{m1}(z_{m1}) + (Ra_{Im1}(2z_{m1} - 1)w_{m1}(z_{m1}) = 0 \quad (35)$$

$$\tau(D_{m1}^2 - a_{m1}^2)\phi_{m1}(z_{m1}) + W_{m1}(z_{m1}) + Sr_{m1}(D_{m1}^2 - a_{m1}^2)\theta_{m1}(z_{m1}) = 0 \quad (36)$$

Where,

$a$  and  $a_{m1}$  are the non dimensional horizontal wave number,  $\frac{\partial}{\partial z} = D_{f1}$  and  $\frac{\partial}{\partial z_{m1}} = D_{m1}$ ,

$\Phi$  and  $\Phi_{m1}$  are the concentrations  $\theta$  and  $\theta_{m1}$  are the temperature in fluid and porous layers respectively.  $W_{f1}$  and  $W_{m1}$  are dimensionless vertical velocity distribution in fluid and porous layers respectively. Boundary conditions at the fluid and porous layer interface have a great effect on the prediction of convection stability in a composite layer. The interface effect also determines the flow pattern, temperature mass distributions and heat transfer rates. Equations (46) to (51) are to be solved subjected to the following appropriate velocity, temperature and concentration boundary conditions.

#### 4. Boundary conditions

##### The velocity boundary conditions are:

At the free surface of the fluid layer,

$$W_{f1}(1) = 0$$

$$D_{f1}^2 W_{f1}(1) + Ma_{Tf1} a^2 \theta(1) + Ma_S a^2 \phi(1) = 0$$

At the rigid surface of the porous layer,

$$W_{m1}(0) = 0$$

At interface,

$$W_{f1}(0) = \frac{\hat{d}}{\hat{k}_{Tf1}} W_{m1}(1)$$

$$D_{f1}^2 W_{f1}(0) = \frac{\hat{d}^3}{\hat{k}_{Tf1}} D_{m1}^2 W_{m1}(1)$$

$$D_{f1}^3 W_{f1}(0) = \frac{\hat{d}^4}{\hat{k}_{Tf1} Da} D_{m1} W_{m1}(1)$$

##### Adiabatic temperature boundary condition:

At the top of the fluid layer,

$$D_{f1}\theta_{f1}(1) = 0$$

At the bottom of the porous layer,

$$D_{m1}\theta_{m1}(0) = 0$$

At interface,

$$\theta_{f1}(0) = \frac{\hat{k}_{Tf1}}{\hat{d}}\theta_{m1}(1)$$

$$D_{f1}\theta_{f1}(0) = D_{m1}\theta_{m1}(1)$$

**Adiabatic concentration boundary condition:**

At the top of the fluid layer

$$D_{f1}\Phi(1) = 0$$

At the bottom of the porous layer

$$D_{m1}\Phi_{m1}(0) = 0$$

At interface

$$\Phi(0) = \frac{\hat{k}_{Cf1}}{\hat{d}}\Phi_{m1}(1)$$

$$D_{f1}\Phi(0) = D_{m1}\Phi_{m1}(1)$$

The system comprising of equations (31) to (33) corresponds to the fluid medium and the system comprising of equations (34) to (36) corresponds to the porous medium along with the boundary conditions, forms an eigenvalue problem with  $Ra_{Tf1}$  being the eigenvalue. Since both systems consist of space varying coefficients. It is no longer possible to obtain a closed form solution of the problem. We therefore use a regular perturbation method to solve the eigenvalue problem.

**5. Method of solution by Regular Perturbation Technique**

An eigen value problem with  $Ra_{Tf1}$  as an eigen value that has to be solved for different salinity gradients. The horizontal wavenumber  $a$  is negligibly small. Hence, the eigen value problem is solved by regular Perturbation technique with wave number  $a$  as a perturbation parameter accordingly, the variables  $W$ ,  $\Phi$  and  $\theta$  expanded in powers of  $a^2$  as,

$$(w_{f1}(z), \theta_{f1}(z), \phi_{f1}(z)) = \sum_{i=0}^{\infty} (a_{f1}^2)^i (W_{f1_i}(z), \theta_{f1_i}(z), \Phi_i(z)) \quad (37)$$

$$(w_{m1}(z_{m1}), \theta_{m1}(z_{m1}), \phi_{m1}(z_{m1}))$$

$$= \sum_{i=0}^{\infty} (a_{m1}^2)^i (W_{m1i}(z_{m1}), \Theta_{m1i}(z_{m1}), \Phi_{m1i}(z_{m1})) \quad (38)$$

Substituting equation (37) and (38) into equation (31) to (36) yields a sequence of equation for the unknown functions.

$W_i(z), W_{m1i}(z_{m1}), \Theta_i(z), \Theta_{m1i}(z_{m1}), \Phi_i(z), \Phi_{m1i}(z_{m1})$  for  $i = 0, 1, 2, 3 \dots$

The zeroth order equations are:

$$D_{f1}^4 W_0(z) = 0$$

$$D_{m1}^2 W_{m0}(z_{m1}) = 0$$

$$D_{f1}^2 \Theta_{f1_0}(z) = 0$$

$$D_{m1}^2 \Theta_{m0}(z_{m1}) = 0$$

$$D_{f1}^2 \Phi_0(z) = 0$$

$$D_{m1}^2 \Phi_{m0}(z_{m1}) = 0$$

The corresponding velocity boundary conditions of zeroth order are:

$$W_0(1) = 0$$

$$D_{f1}^2 W_0(1) = 0$$

$$W_{m0}(0) = 0$$

$$W_0(0) = \frac{\hat{d}}{\hat{k}_{Tf1}} W_{m0}(1)$$

$$D_{f1}^2 W_0(0) = \frac{\hat{d}^3}{\hat{k}_{Tf1}} D_{m1}^2 W_{m0}(1)$$

$$D_{f1}^3 W_0(0) = -\frac{\hat{d}^4}{\hat{k}_{Tf1}} D_{m1} W_{m0}(1)$$

The corresponding adiabatic thermal boundary conditions of zeroth order are:

$$D_{f1} \Theta_{f1_0}(1) = 0$$

$$D_{m1} \Theta_{m0}(1) = 0$$

$$\Theta_{f1_0}(0) = \frac{\hat{k}_{Tf1}}{\hat{d}} \Theta_{m0}(1)$$

$$D_{f1} \Theta_{f1_0}(0) = D_{m1} \Theta_{m0}(0)$$

The corresponding adiabatic concentration boundary conditions of zeroth order are:

$$D_{f1} \Phi_0(1) = 0$$

$$D_{m1} \Phi_{m0}(0) = 0$$

$$\Phi_0(0) = \frac{\hat{k}_{C_{f1}}}{\hat{d}} \Phi_{m0}(1)$$

$$D_{f1} \Phi_0(0) = D_{m1} \Phi_{m0}(1)$$

The solutions at zeroth order equations are:

$$W_0(z) = 0$$

$$W_{m0}(z_{m1}) = 0$$

$$\theta_0(z) = \widehat{T}_{f1}$$

$$\theta_{m0}(z_{m1}) = 1$$

$$\Phi_0(z) = \widehat{C}_{f1}$$

$$\Phi_{m0}(z_{m1}) = 1$$

The equations of first order of  $a^2$  are:

$$D_{f1}^4 W_1(z) = Ra_T \widehat{T}_{f1} - Ra_S \widehat{C}_{f1} \quad (39)$$

$$D_{f1_m}^4 W_{m1}(z_m) = -Ra_{Tm} + Ra_{Sm} \quad (40)$$

$$D_{f1}^2 \theta_1(z) + W_1(z) + R_I(2z - 1)W_1(z) = \widehat{T}_{f1} \quad (41)$$

$$D_m^2 \theta_{m1}(z_m) + W_{m1}(z_m) + R_{Im}(2z_m + 1)W_{m1}(z_m) = 1 \quad (42)$$

$$\tau D_{f1}^2 \Phi_1(z) + W_1(z) + Sr D_{f1}^2 \theta_1(z) = \tau \widehat{C}_{f1} + Sr \widehat{T}_{f1} \quad (43)$$

$$\tau_m D_m^2 \Phi_{m1}(z_m) + W_{m1}(z_m) + Sr_m D_m^2 \theta_{m1}(z_m) = 1 \quad (44)$$

The corresponding velocity boundary conditions of first order of  $a^2$  are:

$$W_1(1) = 0$$

$$D_{f1}^2 W_1(1) + Ma_T \widehat{T}_{f1} + Ma_S \widehat{C}_{f1} = 0$$

$$W_{m1}(0) = 0$$

$$W_1(0) = \frac{1}{\hat{k}_{T_{f1}} \hat{d}} W_m(1)$$

$$D_{f1}^2 W_1(0) = \frac{\hat{d}}{\hat{k}_{T_{f1}}} D_m^2 W_m(1)$$

$$D_{f1}^3 W_1(0) = -\frac{\hat{d}^2}{Da \hat{k}_{T_{f1}}} D_m W_m(1)$$

The solutions to equations (39) and (40) after applying velocity boundary conditions we obtain,

$$W_1(z) = \left\{ \begin{aligned} &\left( A_8 + A_{10}z + A_2z^2 + A_4z^3 + \frac{\widehat{T}_{f1}}{24}z^4 \right) Ra_{T_{f1}} \\ &+ \left( A_7 + A_9z + A_1z^2 + A_3z^3 - \frac{\widehat{C}_{f1}}{24}z^4 \right) Ra_S + \\ &\left( \frac{1}{\widehat{d}\widehat{k}_{T_{f1}}Da} + A_{12}z - \frac{\widehat{T}_{f1}}{6}z^3 \right) Ma_T \\ &+ \left( \frac{\widehat{C}_{f1}}{\widehat{d}\widehat{k}_{T_{f1}}\widehat{T}_{f1}Da} + A_{11}z - \frac{\widehat{C}_{f1}}{6}z^3 \right) Ma_S \end{aligned} \right\} \quad (45)$$

$$W_{m1}(z_{m1}) = \left\{ \begin{aligned} &\left( A_6z_{m1} - \frac{\widehat{T}_{f1}^2 Da}{2}z_{m1}^2 \right) Ra_{T_{f1}} + \left( A_5z_{m1} + \frac{\widehat{C}_{f1}^2 Da}{2}z_{m1}^2 \right) Ra_S \\ &+ \left( \frac{1}{Da}z_{m1} \right) Ma_{T_{f1}} + \left( \frac{\widehat{C}_{f1}}{\widehat{T}_{f1}Da}z_{m1} \right) Ma_S \end{aligned} \right\} \quad (46)$$

Where,

$$\begin{aligned} A_1 &= \frac{\widehat{k}_{C_{f1}}^2 Da}{2\widehat{k}_{T_{f1}}\widehat{d}^3}, & A_2 &= -\frac{\widehat{k}_{T_{f1}} Da}{2\widehat{d}^3}, & A_3 &= -\left( \frac{\widehat{k}_{C_{f1}}}{12\widehat{d}} + \frac{A_1}{3} \right), & A_4 &= -\left( \frac{\widehat{k}_{T_{f1}}}{12\widehat{d}} - \frac{A_2}{3} \right) \\ A_5 &= -\left( \frac{6\widehat{k}_{T_{f1}} Da A_3}{\widehat{d}^2} - \frac{\widehat{k}_{C_{f1}}^2 Da}{\widehat{d}^4} \right), & A_6 &= -\left( \frac{\widehat{k}_{T_{f1}}^2 Da}{\widehat{d}^4} - \frac{6\widehat{k}_{T_{f1}} Da A_4}{\widehat{d}^2} \right) \\ A_7 &= -\left( \frac{A_5}{\widehat{d}\widehat{k}_{T_{f1}}} + \frac{\widehat{k}_{C_{f1}}^2 Da}{2\widehat{k}_{T_{f1}}\widehat{d}^5} \right), & A_8 &= \left( \frac{A_6}{\widehat{d}\widehat{k}_{T_{f1}}} - \frac{\widehat{k}_{T_{f1}} Da}{2\widehat{d}^5} \right) \\ A_9 &= -A_7 - A_1 - A_3 + \frac{\widehat{k}_{C_{f1}}}{12\widehat{d}}, & A_{10} &= -A_8 - A_2 - A_4 - \frac{\widehat{k}_{T_{f1}}}{24\widehat{d}} \end{aligned}$$

## 6. Compatibility condition

Compatibility condition is obtained by integrating the temperature and the concentration equations. Integrating temperature and concentrations equations (41) and (43) between  $z=0$  and  $z=1$ , and multiplying equation (43) and (44) by  $\frac{1}{\widehat{d}^2}$  and integrate between  $z_{m1} = 0$  and  $z_{m1} = 1$  and adding the resulting equations, we obtain the compatibility condition as,

$$\left\{ \begin{aligned} & \frac{Sr}{\tau} (1 - R_l) \int_0^1 W_1 f(z) dz + \frac{2R_l Sr}{\tau} (1 - R_l) \int_0^1 z W_1 f(z) dz \\ & + \frac{Sr_m (1 + R_{lm})}{\tau_m \hat{d}^2} \int_0^1 W_{m1} f_m(z_m) dz_m \\ & - \frac{1}{\tau} \int_0^1 W_1 g(z) dz - \frac{1}{\tau_m \hat{d}^2} \int_0^1 W_{m1} g_m(z_m) dz_m \\ & + \frac{2R_{lm} Sr_m}{\tau_m \hat{d}^2} \int_0^1 z_m W_{m1} f_m(z_m) dz_m \end{aligned} \right\} = -\frac{\hat{k}_c}{\hat{d}} - \frac{1}{\hat{d}^2} \quad (47)$$

By substituting the expression for  $W_1$  and  $W_m$  from equations (45) and (46) into the equation (47) and we obtain an expression for critical Rayleigh number.

### Linear Salinity Gradient (LSG):

For linear salinity Gradient  $f(z) = f_{m1}(z_{m1}) = 1$ , substituting the expression for  $W_1$  and  $W_{m1}$  into the equation (47), integrating and solving we obtain critical Rayleigh number  $Rc_1$ .

$$Rc_1 = \frac{\Sigma - \Pi_1 Ra_s - \Pi_2 Ma_{T_{f1}} - \Pi_3 Ma_s}{\Pi_4}$$

Where,

$$\Pi_1 = (B_2 + B_6 + B_{10} + B_{14} + B_{18} + B_{22})$$

$$\Pi_2 = (B_3 + B_7 + B_{11} + B_{15} + B_{19} + B_{23})$$

$$\Pi_3 = (B_4 + B_8 + B_{12} + B_{16} + B_{20} + B_{23})$$

$$\Pi_4 = (B_4 + B_5 + B_9 + B_{13} + B_{17} + B_{21})$$

$$B_1 = \frac{Sr}{\tau} (1 - R_l) \left( \frac{A_{10}}{2} + \frac{A_2}{3} + \frac{A_4}{4} + A_8 + \frac{\hat{k}_{T_{f1}}}{120 d} \right)$$

;

$$B_1 = \frac{Sr}{\tau} (1 - R_l) \left( \frac{A_{10}}{2} + \frac{A_2}{3} + \frac{A_4}{4} + A_8 + \frac{\hat{k}_{T_{f1}}}{120 d} \right)$$

$$B_2 = \frac{Sr}{\tau} (1 - R_l) \left( \frac{A_9}{2} + \frac{A_1}{3} + \frac{A_3}{4} + A_7 - \frac{\hat{k}_{C_{f1}}}{120 d} \right)$$

$$B_3 = -\frac{(-1 + R_l) Sr}{24 d^2 \tau} (12 + d k_{T_{f1}})$$

$$B_4 = -\frac{(-1 + R_l) Sr k_{C_{f1}}}{8 d^2 \tau k_{T_{f1}}} (-12 + d k_{T_{f1}})$$

$$B_5 = \frac{R_l Sr}{\tau} \left( \frac{2A_{10}}{3} + \frac{A_2}{2} + \frac{2A_4}{5} + A_8 + \frac{\hat{k}_{T_{f1}}}{72 d} \right)$$

$$\begin{aligned}
 B_7 &= \frac{R_I S r}{3d^2 \tau} + \frac{2k_{T_{f1}} R_I S r}{45 d \tau}; & B_8 &= \frac{5K_{C_{f1}} R_I S r}{3d^2 k_{T_{f1}} \tau} - \frac{8k_{C_{f1}} R_I S r}{45 d \tau}; \\
 B_9 &= \frac{(1 + R_{Im1}) S r_{m1} (3A_6 d^4 - Dak_{T_{f1}}^2)}{6d^6 \tau_{m1}}; & B_{10} &= \frac{(1 + R_{Im1}) S r_{m1} (3A_5 d^4 - Dak_{C_{f1}}^2)}{6d^6 \tau_{m1}} \\
 B_{11} &= \frac{k_{T_{f1}} S r_{m1}}{2d^3 \tau_{m1}} + \frac{k_{T_{f1}} R_{Im1} S r_{m1}}{2d^3 \tau_{m1}}; & B_{12} &= \frac{k_{C_{f1}} S r_{m1}}{2d^3 \tau_{m1}} + \frac{k_C R_{Im1} S r_{m1}}{2d^3 \tau_{m1}} \\
 B_{13} &= \frac{2A_6 R_{Im1} S r_{m1}}{3d^2 \tau_{m1}} - \frac{Dak_{T_{f1}}^2 R_{Im1} S r_{m1}}{4d^6 \tau_{m1}}; & B_{14} &= \frac{2A_5 R_{Im1} S r_{m1}}{3d^2 \tau_{m1}} - \frac{Dak_{C_{f1}}^2 R_{Im1} S r_{m1}}{4d^6 \tau_{m1}} \\
 B_{15} &= \frac{2k_{T_{f1}} R_{Im1} S r_{m1}}{3d^3 \tau_{m1}}; & B_{16} &= \frac{2k_{C_{f1}} R_{Im1} S r_{m1}}{3d^3 \tau_{m1}} \\
 B_{17} &= -\frac{1}{\tau} \left( \frac{A_{10}}{2} + \frac{A_2}{3} + \frac{A_4}{4} + A_8 + \frac{\hat{k}_{T_{f1}}}{120 d} \right); \\
 B_{18} &= -\frac{1}{\tau} \left( \frac{A_9}{2} + \frac{A_1}{3} + \frac{A_3}{4} + A_7 - \frac{\hat{k}_{C_{f1}}}{120 d} \right) \\
 B_{20} &= -\frac{k_{C_{f1}}}{8 d \tau} - \frac{3k_{C_{f1}}}{2d^2 k_{T_{f1}} \tau}; & B_{21} &= -\frac{A_6}{2d^2 \tau_{m1}} + \frac{Dak_{T_{f1}}^2}{6d^6 \tau_{m1}}; \\
 B_{22} &= -\frac{A_5}{2d^2 \tau_{m1}} + \frac{Dak_{C_{f1}}^2}{6d^6 \tau_{m1}}; & B_{23} &= -\frac{k_{T_{f1}}}{2 d^3 \tau_{m1}}; & B_{24} &= -\frac{k_{C_{f1}}}{2 d^3 \tau_{m1}}
 \end{aligned}$$

### Parabolic Salinity Gradient (PSG):

For parabolic salinity Gradient  $f(z) = 2z$  and  $f_{m1}(z_{m1}) = 2z_{m1}$ , substituting the expression for  $W_1$  and  $W_{m1}$  into the equation (47), integrating and solving for critical Rayleigh number  $Rc_2$  and is obtained in the form,

$$Rc_2 = \frac{\Sigma - \Pi_5 Ra_S - \Pi_6 Ma_T - \Pi_7 Ma_S}{\Pi_8}$$

Where,

$$\Pi_5 = (B_2 + B_6 + B_{10} + B_{14} + B_{18} + B_{22})$$

$$\Pi_6 = (B_3 + B_7 + B_{11} + B_{15} + B_{19} + B_{23})$$

$$\Pi_7 = (B_4 + B_8 + B_{12} + B_{16} + B_{20} + B_{23})$$

$$\Pi_8 = (B_4 + B_5 + B_9 + B_{13} + B_{17} + B_{21})$$

$$B_1 = \frac{Sr}{\tau} (1 - R_I) \left( \frac{A_{10}}{2} + \frac{A_2}{3} + \frac{A_4}{4} + A_8 + \frac{\hat{k}_T}{120 d} \right)$$

$$B_2 = \frac{Sr}{\tau} (1 - R_I) \left( \frac{A_9}{2} + \frac{A_1}{3} + \frac{A_3}{4} + A_7 - \frac{\hat{k}_C}{120 d} \right)$$

$$B_3 = -\frac{(-1 + R_I)Sr}{24d^2\tau} (12 + dk_{T_{f1}})$$

$$B_4 = -\frac{(-1 + R_I)Sr k_C}{8d^2\tau k_{T_{f1}}} (-12 + d k_{T_{f1}})$$

$$B_5 = \frac{R_I Sr}{\tau} \left( \frac{2A_{10}}{3} + \frac{A_2}{2} + \frac{2A_4}{5} + A_8 + \frac{\hat{k}_{T_{f1}}}{72 d} \right)$$

$$B_6 = -\frac{R_I Sr}{\tau} \left( \frac{2A_9}{3} + \frac{A_1}{2} + \frac{2A_3}{5} + A_7 - \frac{\hat{k}_C}{72 d} \right)$$

$$B_7 = \frac{R_I Sr}{3d^2\tau} + \frac{2k_{T_{f1}} R_I Sr}{45 d\tau}; \quad B_8 = \frac{5K_C R_I Sr}{3d^2 k_{T_{f1}} \tau} - \frac{8k_C R_I Sr}{45 d\tau}$$

$$B_9 = \frac{(1 + R_{Im})Sr_m(3A_6d^4 - Dak_{T_{f1}}^2)}{6d^6\tau_m}; \quad B_{10} = \frac{(1 + R_{Im})Sr_m(3A_5d^4 - Dak_C^2)}{6d^6\tau_m}$$

$$B_{11} = \frac{k_{T_{f1}} Sr_m}{2d^3\tau_m} + \frac{k_{T_{f1}} R_{Im} Sr_m}{2d^3\tau_m}; \quad B_{12} = \frac{k_C Sr_m}{2d^3\tau_m} + \frac{k_C R_{Im} Sr_m}{2d^3\tau_m}$$

$$B_{13} = \frac{2A_6 R_{Im} Sr_m}{3d^2\tau_m} - \frac{Dak_T^2 R_{Im} Sr_m}{4d^6\tau_m}; \quad B_{14} = \frac{2A_5 R_{Im} Sr_m}{3d^2\tau_m} - \frac{Dak_C^2 R_{Im} Sr_m}{4d^6\tau_m}$$

$$B_{15} = \frac{2k_{T_{f1}} R_{Im} Sr_m}{3d^3\tau_m}; \quad B_{16} = \frac{2k_C R_{Im} Sr_m}{3d^3\tau_m}; \quad B_{17}$$

$$= -\frac{1}{\tau} \left( \frac{A_{10}}{2} + \frac{A_2}{3} + \frac{A_4}{4} + A_8 + \frac{\hat{k}_{T_{f1}}}{120 d} \right)$$

$$B_{18} = -\frac{1}{\tau} \left( \frac{A_9}{2} + \frac{A_1}{3} + \frac{A_3}{4} + A_7 - \frac{\hat{k}_C}{120 d} \right); \quad B_{19} = -\frac{1}{2d^2\tau} - \frac{k_{T_{f1}}}{24 d\tau};$$

$$B_{20} = -\frac{k_C}{8 d\tau} - \frac{3k_C}{2d^2 k_{T_{f1}} \tau}; \quad B_{21} = -\frac{A_6}{2d^2\tau_m} + \frac{Dak_{T_{f1}}^2}{6d^6\tau_m};$$

$$B_{22} = -\frac{A_5}{2d^2\tau_m} + \frac{Dak_C^2}{6d^6\tau_m}; \quad B_{23} = -\frac{k_{T_{f1}}}{2 d^3\tau_m}; \quad B_{24} = -\frac{k_C}{2 d^3\tau_m}$$

### Inverted Parabolic Salinity Gradient (ISG):

For Inverted salinity Gradient  $f(z) = 2(1 - z)$  and  $f_m(z_m) = 2(1 - z_m)$ , integrating and

solving the expression for  $W_1$  and  $W_{m1}$  into the equation (47), integrating and solving for critical Rayleigh number  $Rc_3$  and is obtained in the form,

$$Rc_3 = \frac{\Sigma - \Pi_9 Ra_S - \Pi_{10} Ma_{Tf1} - \Pi_{11} Ma_S}{\Pi_{12}}$$

Where,

$$\Pi_9 = (B_2 + B_6 + B_{10} + B_{14} + B_{18} + B_{22})$$

$$\Pi_{10} = (B_3 + B_7 + B_{11} + B_{15} + B_{19} + B_{23})$$

$$\Pi_{11} = (B_4 + B_8 + B_{12} + B_{16} + B_{20} + B_{23})$$

$$\Pi_{12} = (B_4 + B_5 + B_9 + B_{13} + B_{17} + B_{21})$$

$$B_1 = \frac{Sr}{\tau} (1 - R_I) \left( \frac{A_{10}}{2} + \frac{A_2}{3} + \frac{A_4}{4} + A_8 + \frac{\hat{k}_T}{120 d} \right)$$

$$B_2 = \frac{Sr}{\tau} (1 - R_I) \left( \frac{A_9}{2} + \frac{A_1}{3} + \frac{A_3}{4} + A_7 - \frac{\hat{k}_C}{120 d} \right)$$

$$B_3 = -\frac{(-1 + R_I)Sr}{24d^2\tau} (12 + dk_T); \quad B_4 = -\frac{(-1 + R_I)Sr k_C}{8d^2\tau k_T} (-12 + d k_T);$$

$$B_5 = \frac{R_I Sr}{\tau} \left( \frac{2A_{10}}{3} + \frac{A_2}{2} + \frac{2A_4}{5} + A_8 + \frac{\hat{k}_T}{72 d} \right); \quad B_6 = -\frac{R_I Sr}{\tau} \left( \frac{2A_9}{3} + \frac{A_1}{2} + \frac{2A_3}{5} + A_7 - \frac{\hat{k}_C}{72 d} \right);$$

$$B_7 = \frac{R_I Sr}{3d^2\tau} + \frac{2k_T R_I Sr}{45 d\tau}; \quad B_8 = \frac{5K_C R_I Sr}{3d^2 k_T \tau} - \frac{8k_C R_I Sr}{45 d\tau}; \quad B_9 =$$

$$= \frac{(1 + R_{Im})Sr_m (3A_6 d^4 - Dak_T^2)}{6d^6\tau_m}$$

$$B_{10} = \frac{(1 + R_{Im})Sr_m (3A_5 d^4 - Dak_C^2)}{6d^6\tau_m}; \quad B_{11} = \frac{k_T Sr_m}{2d^3\tau_m} + \frac{k_T R_{Im} Sr_m}{2d^3\tau_m};$$

$$B_{12} = \frac{k_C Sr_m}{2d^3\tau_m} + \frac{k_C R_{Im} Sr_m}{2d^3\tau_m}; \quad B_{13} = \frac{2A_6 R_{Im} Sr_m}{3d^2\tau_m} - \frac{Dak_T^2 R_{Im} Sr_m}{4d^6\tau_m};$$

$$B_{14} = \frac{2A_5 R_{Im} Sr_m}{3d^2\tau_m} - \frac{Dak_C^2 R_{Im} Sr_m}{4d^6\tau_m}; \quad B_{15} = \frac{2k_T R_{Im} Sr_m}{3d^3\tau_m};$$

$$B_{16} = \frac{2k_C R_{Im} Sr_m}{3d^3\tau_m}; \quad B_{17} = -\frac{1}{\tau} \left( \frac{A_{10}}{2} + \frac{A_2}{3} + \frac{A_4}{4} + A_8 + \frac{\hat{k}_T}{120 d} \right);$$

$$B_{18} = -\frac{1}{\tau} \left( \frac{A_9}{2} + \frac{A_1}{3} + \frac{A_3}{4} + A_7 - \frac{\hat{k}_C}{120 d} \right); \quad B_{19} = -\frac{1}{2d^2\tau} - \frac{k_T}{24 d\tau};$$

$$B_{20} = -\frac{k_C}{8 d \tau} - \frac{3k_C}{2d^2 k_T \tau}; \quad B_{21} = -\frac{A_6}{2d^2 \tau_m} + \frac{Dak_T^2}{6d^6 \tau_m};$$

$$B_{22} = -\frac{A_5}{2d^2 \tau_m} + \frac{Dak_C^2}{6d^6 \tau_m}; \quad B_{23} = -\frac{k_T}{2 d^3 \tau_m}; \quad B_{24} = -\frac{k_C}{2 d^3 \tau_m}$$

**Piecewise Linear Heated From Below Salinity Gradient (SBSG):**

For piecewise linear heated from below salinity gradient

$$f(z) = \begin{cases} \frac{1}{\varepsilon}, & 0 \leq z \leq \varepsilon_m \\ 0, & \varepsilon \leq z \leq 1 \end{cases} \text{ and } f_m(z_m) = \begin{cases} \frac{1}{\varepsilon_m}, & 0 \leq z_m \leq \varepsilon_m \\ 0, & \varepsilon_m \leq z_m \leq 1 \end{cases}$$

into the equation (47), integrating and solving for critical Rayleigh number  $Rc_4$  and is obtained in the form,

$$Rc_4 = \frac{\Sigma - \Pi_{13} Ra_S - \Pi_{14} Ma_T - \Pi_{15} Ma_S}{\Pi_{16}}$$

Where,

$$\Pi_{13} = (B_2 + B_6 + B_{10} + B_{14} + B_{18} + B_{22})$$

$$\Pi_{14} = (B_3 + B_7 + B_{11} + B_{15} + B_{19} + B_{23})$$

$$\Pi_{15} = (B_4 + B_8 + B_{12} + B_{16} + B_{20} + B_{23})$$

$$\Pi_{16} = (B_4 + B_5 + B_9 + B_{13} + B_{17} + B_{21})$$

$$B_1 = \frac{Sr}{\tau} (1 - R_I) \left( \frac{A_{10}}{2} + \frac{A_2}{3} + \frac{A_4}{4} + A_8 + \frac{\hat{k}_T}{120 d} \right)$$

$$B_2 = \frac{Sr}{\tau} (1 - R_I) \left( \frac{A_9}{2} + \frac{A_1}{3} + \frac{A_3}{4} + A_7 - \frac{\hat{k}_C}{120 d} \right)$$

;

$$B_3 = -\frac{(-1 + R_I)Sr}{24d^2 \tau} (12 + dk_T); \quad B_4 = -\frac{(-1 + R_I)Sr k_C}{8d^2 \tau k_T} (-12 + d k_T);$$

$$B_5 = \frac{R_I Sr}{\tau} \left( \frac{2A_{10}}{3} + \frac{A_2}{2} + \frac{2A_4}{5} + A_8 + \frac{\hat{k}_T}{72 d} \right);$$

$$B_6 = -\frac{R_I Sr}{\tau} \left( \frac{2A_9}{3} + \frac{A_1}{2} + \frac{2A_3}{5} + A_7 - \frac{\hat{k}_C}{72 d} \right); \quad B_7 = \frac{R_I Sr}{3d^2 \tau} + \frac{2k_T R_I Sr}{45 d \tau};$$

$$B_8 = \frac{5K_C R_I Sr}{3d^2 k_T \tau} - \frac{8k_C R_I Sr}{45 d \tau}; \quad B_9 = \frac{(1 + R_{Im})Sr_m (3A_6 d^4 - Dak_T^2)}{6d^6 \tau_m}$$

$$\begin{aligned}
 B_{10} &= \frac{(1 + R_{Im})Sr_m(3A_5d^4 - Dak_C^2)}{6d^6\tau_m}; & B_{11} &= \frac{k_T Sr_m}{2d^3\tau_m} + \frac{k_T R_{Im} Sr_m}{2d^3\tau_m}; \\
 B_{12} &= \frac{k_C Sr_m}{2d^3\tau_m} + \frac{k_C R_{Im} Sr_m}{2d^3\tau_m}; & B_{13} &= \frac{2A_6 R_{Im} Sr_m}{3d^2\tau_m} - \frac{Dak_T^2 R_{Im} Sr_m}{4d^6\tau_m}; \\
 B_{14} &= \frac{2A_5 R_{Im} Sr_m}{3d^2\tau_m} - \frac{Dak_C^2 R_{Im} Sr_m}{4d^6\tau_m}; & B_{15} &= \frac{2k_T R_{Im} Sr_m}{3d^3\tau_m}; \\
 B_{16} &= \frac{2k_C R_{Im} Sr_m}{3d^3\tau_m}; & B_{17} &= -\frac{1}{\tau} \left( \frac{A_{10}}{2} + \frac{A_2}{3} + \frac{A_4}{4} + A_8 + \frac{\hat{k}_T}{120d} \right); \\
 B_{18} &= -\frac{1}{\tau} \left( \frac{A_9}{2} + \frac{A_1}{3} + \frac{A_3}{4} + A_7 - \frac{\hat{k}_C}{120d} \right); & B_{19} &= -\frac{1}{2d^2\tau} - \frac{k_T}{24d\tau}; \\
 B_{20} &= -\frac{k_C}{8d\tau} - \frac{3k_C}{2d^2k_T\tau}; & B_{21} &= -\frac{A_6}{2d^2\tau_m} + \frac{Dak_T^2}{6d^6\tau_m}; \\
 B_{22} &= -\frac{A_5}{2d^2\tau_m} + \frac{Dak_C^2}{6d^6\tau_m}; & B_{23} &= -\frac{k_T}{2d^3\tau_m}; & B_{24} &= -\frac{k_C}{2d^3\tau_m}
 \end{aligned}$$

### Piecewise Linear Cooling From Above Salinity Gradient (SASG):

For piecewise linear cooled from below salinity gradient

$$f(z) = \begin{cases} 0, & 0 \leq z < 1 - \varepsilon \\ \frac{1}{\varepsilon}, & 1 - \varepsilon \leq z \leq 1 \end{cases} \text{ and } f_m(z_m) = \begin{cases} 0, & 0 \leq z_m < 1 - \varepsilon_m \\ \frac{1}{\varepsilon_m}, & 1 - \varepsilon_m \leq z_m \leq 1 \end{cases}$$

Into the equation (47), integrating and solving for critical Rayleigh number  $Rc_5$  and is obtained in the form,

$$Rc_5 = \frac{\Sigma - \Pi_{17} Ra_S - \Pi_{18} Ma_T - \Pi_{19} Ma_S}{\Pi_{20}}$$

Where,

$$\Pi_{17} = (B_2 + B_6 + B_{10} + B_{14} + B_{18} + B_{22})$$

$$\Pi_{18} = (B_3 + B_7 + B_{11} + B_{15} + B_{19} + B_{23})$$

$$\Pi_{19} = (B_4 + B_8 + B_{12} + B_{16} + B_{20} + B_{23})$$

$$\Pi_{20} = (B_4 + B_5 + B_9 + B_{13} + B_{17} + B_{21})$$

$$B_1 = \frac{Sr}{\tau} (1 - R_l) \left( \frac{A_{10}}{2} + \frac{A_2}{3} + \frac{A_4}{4} + A_8 + \frac{\hat{k}_T}{120d} \right)$$

$$B_2 = \frac{Sr}{\tau} (1 - R_l) \left( \frac{A_9}{2} + \frac{A_1}{3} + \frac{A_3}{4} + A_7 - \frac{\hat{k}_C}{120d} \right)$$

$$\begin{aligned}
 B_3 &= -\frac{(-1 + R_l)Sr}{24d^2\tau} (12 + dk_T); & B_4 &= -\frac{(-1 + R_l)Sr k_C}{8d^2\tau k_T} (-12 + d k_T); \\
 B_5 &= \frac{R_l Sr}{\tau} \left( \frac{2A_{10}}{3} + \frac{A_2}{2} + \frac{2A_4}{5} + A_8 + \frac{\hat{k}_T}{72 d} \right); \\
 B_6 &= -\frac{R_l Sr}{\tau} \left( \frac{2A_9}{3} + \frac{A_1}{2} + \frac{2A_3}{5} + A_7 - \frac{\hat{k}_C}{72 d} \right); & B_7 &= \frac{R_l Sr}{3d^2\tau} + \frac{2k_T R_l Sr}{45 d\tau}; \\
 B_8 &= \frac{5K_C R_l Sr}{3d^2 k_T \tau} - \frac{8k_C R_l Sr}{45 d\tau}; & B_9 &= \frac{(1 + R_{Im})Sr_m (3A_6 d^4 - Dak_T^2)}{6d^6 \tau_m}; \\
 B_{10} &= \frac{(1 + R_{Im})Sr_m (3A_5 d^4 - Dak_C^2)}{6d^6 \tau_m}; & B_{11} &= \frac{k_T Sr_m}{2d^3 \tau_m} + \frac{k_T R_{Im} Sr_m}{2d^3 \tau_m}; \\
 B_{12} &= \frac{k_C Sr_m}{2d^3 \tau_m} + \frac{k_C R_{Im} Sr_m}{2d^3 \tau_m}; & B_{13} &= \frac{2A_6 R_{Im} Sr_m}{3d^2 \tau_m} - \frac{Dak_T^2 R_{Im} Sr_m}{4d^6 \tau_m}; \\
 B_{14} &= \frac{2A_5 R_{Im} Sr_m}{3d^2 \tau_m} - \frac{Dak_C^2 R_{Im} Sr_m}{4d^6 \tau_m}; & B_{15} &= \frac{2k_T R_{Im} Sr_m}{3d^3 \tau_m}; \\
 B_{16} &= \frac{2k_C R_{Im} Sr_m}{3d^3 \tau_m}; & B_{17} &= -\frac{1}{\tau} \left( \frac{A_{10}}{2} + \frac{A_2}{3} + \frac{A_4}{4} + A_8 + \frac{\hat{k}_T}{120 d} \right); \\
 B_{18} &= -\frac{1}{\tau} \left( \frac{A_9}{2} + \frac{A_1}{3} + \frac{A_3}{4} + A_7 - \frac{\hat{k}_C}{120 d} \right); & B_{19} &= -\frac{1}{2d^2\tau} - \frac{k_T}{24 d\tau}; \\
 B_{20} &= -\frac{k_C}{8 d\tau} - \frac{3k_C}{2d^2 k_T \tau}; & B_{21} &= -\frac{A_6}{2d^2 \tau_m} + \frac{Dak_T^2}{6d^6 \tau_m}; \\
 B_{22} &= -\frac{A_5}{2d^2 \tau_m} + \frac{Dak_C^2}{6d^6 \tau_m}; & B_{23} &= -\frac{k_T}{2 d^3 \tau_m}; & B_{24} &= -\frac{k_C}{2 d^3 \tau_m}
 \end{aligned}$$

### Step Function Salinity Gradient (SFSG) :

For step function salinity gradient  $f(z) = f(\varepsilon)$  and  $f_m(z_m) = f(\varepsilon_m)$  into the equation (47), integrating and solving for critical Rayleigh number  $Rc_6$  and is obtained in the form,

$$Rc_6 = \frac{\sum - \Pi_{21} Ra_S - \Pi_{22} Ma_T - \Pi_{23} Ma_S}{\Pi_{24}}$$

Where,

$$\begin{aligned}
 \Pi_{21} &= (B_2 + B_6 + B_{10} + B_{14} + B_{18} + B_{22}) \\
 \Pi_{22} &= (B_3 + B_7 + B_{11} + B_{15} + B_{19} + B_{23}) \\
 \Pi_{23} &= (B_4 + B_8 + B_{12} + B_{16} + B_{20} + B_{23}) \\
 \Pi_{24} &= (B_4 + B_5 + B_9 + B_{13} + B_{17} + B_{21}) \\
 B_1 &= \frac{Sr}{\tau} (1 - R_l) \left( \frac{A_{10}}{2} + \frac{A_2}{3} + \frac{A_4}{4} + A_8 + \frac{\hat{k}_T}{120 d} \right)
 \end{aligned}$$

$$\begin{aligned}
 B_2 &= \frac{Sr}{\tau} (1 - R_I) \left( \frac{A_9}{2} + \frac{A_1}{3} + \frac{A_3}{4} + A_7 - \frac{\hat{k}_C}{120 d} \right) \\
 B_3 &= -\frac{(-1 + R_I)Sr}{24d^2\tau} (12 + dk_T); & B_4 &= -\frac{(-1 + R_I)Sr k_C}{8d^2\tau k_T} (-12 + d k_T); \\
 B_5 &= \frac{R_I Sr}{\tau} \left( \frac{2A_{10}}{3} + \frac{A_2}{2} + \frac{2A_4}{5} + A_8 + \frac{\hat{k}_T}{72 d} \right); \\
 B_6 &= -\frac{R_I Sr}{\tau} \left( \frac{2A_9}{3} + \frac{A_1}{2} + \frac{2A_3}{5} + A_7 - \frac{\hat{k}_C}{72 d} \right); & B_7 &= \frac{R_I Sr}{3d^2\tau} + \frac{2k_T R_I Sr}{45 d\tau}; \\
 B_8 &= \frac{5K_C R_I Sr}{3d^2 k_T \tau} - \frac{8k_C R_I Sr}{45 d\tau}; & B_9 &= \frac{(1 + R_{Im}) Sr_m (3A_6 d^4 - Dak_T^2)}{6d^6 \tau_m} \\
 B_{10} &= \frac{(1 + R_{Im}) Sr_m (3A_5 d^4 - Dak_C^2)}{6d^6 \tau_m}; & B_{11} &= \frac{k_T Sr_m}{2d^3 \tau_m} + \frac{k_T R_{Im} Sr_m}{2d^3 \tau_m}; \\
 B_{12} &= \frac{k_C Sr_m}{2d^3 \tau_m} + \frac{k_C R_{Im} Sr_m}{2d^3 \tau_m}; & B_{13} &= \frac{2A_6 R_{Im} Sr_m}{3d^2 \tau_m} - \frac{Dak_T^2 R_{Im} Sr_m}{4d^6 \tau_m}; \\
 B_{14} &= \frac{2A_5 R_{Im} Sr_m}{3d^2 \tau_m} - \frac{Dak_C^2 R_{Im} Sr_m}{4d^6 \tau_m}; & B_{15} &= \frac{2k_T R_{Im} Sr_m}{3d^3 \tau_m}; \\
 B_{16} &= \frac{2k_C R_{Im} Sr_m}{3d^3 \tau_m}; & B_{17} &= -\frac{1}{\tau} \left( \frac{A_{10}}{2} + \frac{A_2}{3} + \frac{A_4}{4} + A_8 + \frac{\hat{k}_T}{120 d} \right); \\
 B_{18} &= -\frac{1}{\tau} \left( \frac{A_9}{2} + \frac{A_1}{3} + \frac{A_3}{4} + A_7 - \frac{\hat{k}_C}{120 d} \right); & B_{19} &= -\frac{1}{2d^2\tau} - \frac{k_T}{24 d\tau}; \\
 B_{20} &= -\frac{k_C}{8 d\tau} - \frac{3k_C}{2d^2 k_T \tau}; & B_{21} &= -\frac{A_6}{2d^2 \tau_m} + \frac{Dak_T^2}{6d^6 \tau_m}; \\
 B_{22} &= -\frac{A_5}{2d^2 \tau_m} + \frac{Dak_C^2}{6d^6 \tau_m}; & B_{23} &= -\frac{k_T}{2 d^3 \tau_m}; & B_{24} &= -\frac{k_C}{2 d^3 \tau_m}
 \end{aligned}$$

## Results and Discussion

The effect of linear (Rc<sub>1</sub>), parabolic (Rc<sub>2</sub>), inverted parabolic (Rc<sub>3</sub>), salted from below (Rc<sub>4</sub>), salted from above (Rc<sub>5</sub>), and step function (Rc<sub>6</sub>) salinity gradients on the onset of Rayleigh Benard Marangoni convection in a composite layer is analyzed. The variation of Rayleigh number as a function of depth ratio, for different values of the parameter such as solute Rayleigh number, Soret number, Darcy number, thermal Marangoni number, solute Marangoni number, internal Rayleigh number, thermal diffusivity ratio, solute diffusivity ratio and the ratio of

solute to thermal diffusivity are computed and the results are depicted in graphically. The fixed the value of the parameters are  $Da = 0.03, M_{aT} = 5, M_{aS} = 5, R_I = 0.1, S_r = 0.5, R_{aS} = 100, \kappa^T = 1.0, \kappa^C = 1.0$  and  $\tau = 0.3$ .

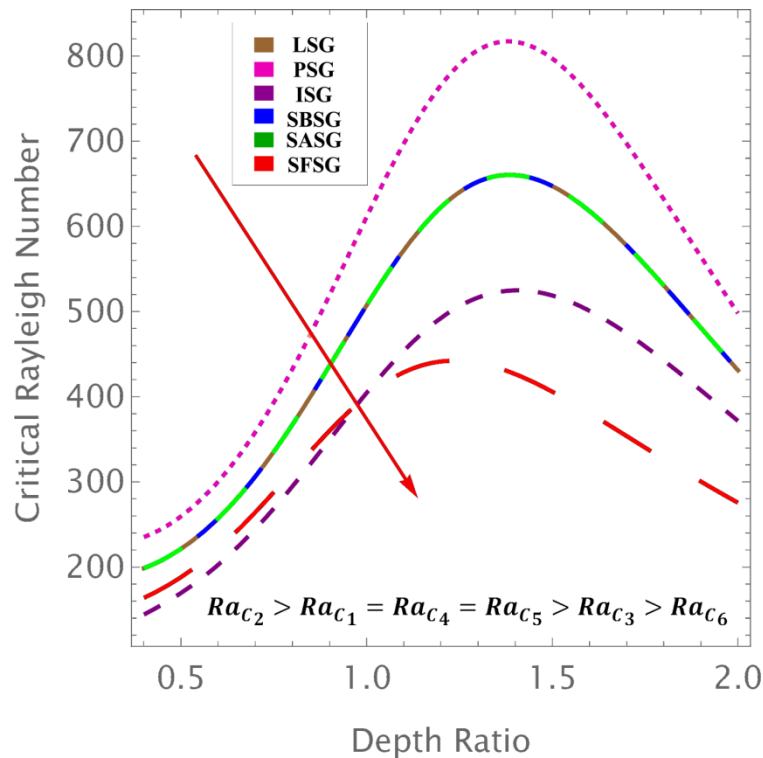


Figure 1: The combined effect of LSG, PSG, ISG, SBSG, SASG, SFSG.

**Figure (2)** depicts the distinction of critical Rayleigh numbers for linear, parabolic, and inverted parabolic, salted from below, salted from above, and step function salinity gradients with depth ratio for various values of the Darcy number  $Da = 0.03, Da = 0.04,$  and  $Da = 0.05$ . The other dimensionless parameters are fixed as

$$M_{aT} = 5, M_{aS} = 5, R_I = 0.1, S_r = 0.5, R_{aS} = 100, \hat{\kappa}_T = 1.0, \hat{\kappa}_C = 1. \text{ and } \tau = 0.3$$

observe that the increase in  $Da$  decreases  $Ra_C$  for all six salinity gradients. An increase in  $Da$  increases the permeability of the porous layer, which facilitates the flow of the fluid and promotes the onset of convection. Hence, the increase in  $Da$  destabilizes the onset of Rayleigh-Benard Marangoni convection. **Figure (3)** depicts the distinction of critical Rayleigh numbers for linear, parabolic, and inverted parabolic salted from below, salted from above, and step function salinity gradients

with depth ratio for various values of the solute diffusivity ratio  $\hat{\kappa}_C = 0.8, 0.9$  and  $1$ . The other dimensionless parameters are fixed as  $Da = 0.03, M_{aT} = 5, M_{aS} = 5, R_I = 0.1, S_r = 0.5, R_{aS} = 100, \hat{\kappa}_T = 1.0$ , and  $\tau = 0.3$ . We observe that the increase in  $\hat{\kappa}_C$  increases  $Ra_C$  for all salinity gradients. An increase in  $\hat{\kappa}_C$  increases solute diffusivity increases concentration of the fluid hence declines the onset of convection. Hence, the increase in  $\hat{\kappa}_C$  stabilizes the onset of Rayleigh-Benard Marangoni convection. **Figure (4)** depicts the distinction of critical Rayleigh numbers for linear, parabolic, and inverted parabolic, salted from below, salted from above, and step function salinity gradients with depth ratio for various values of the thermal diffusivity ratio  $\hat{\kappa}_T = 0.8, \hat{\kappa}_T = 0.9$ , and  $\hat{\kappa}_T = 1.0$ . The other dimensionless parameters are fixed as  $Da = 0.03, M_{aT} = 5, M_{aS} = 5, R_I = 0.1, S_r = 0.5, R_{aS} = 100, \hat{\kappa}_T = 1.0$ , and  $\tau = 0.3$ . We observe that the increase in  $\hat{\kappa}_T$  decreases  $Ra_C$  for all salinity gradients. An increase in  $\hat{\kappa}_T$  increases thermal diffusivity increases temperature gradients in the system which hastens the onset of convection. Hence, the increase in  $\hat{\kappa}_T$  destabilizes the onset of Rayleigh-Benard Marangoni convection. **Figure (5)** depicts the distinction of critical Rayleigh numbers for linear, parabolic, and inverted parabolic salted from below, salted from above, and step function salinity gradients with depth ratio for various values of the thermal Marangoni number  $Ma_s = 5, Ma_s = 10$ , and  $Ma_s = 15$ . The other dimensionless parameters are fixed as  $Da = 0.03, M_{aT} = 5, M_{aS} = 5, R_I = 0.1, S_r = 0.5, R_{aS} = 100, \hat{\kappa}_T = 1.0$ , and  $\tau = 0.3$ . We observe that the increase in  $Ma_s$  increases  $Ra_C$  for all six salinity gradients. An increase in  $Ma_s$  increases the surface tension of the fluid due to solute concentration, which declines the onset of convection. Hence, the increase in  $Ma_s$  stabilizes the onset of Rayleigh-Benard Marangoni convection. **Figure (6)** depicts the distinction of critical Rayleigh numbers for linear, parabolic, and inverted parabolic salted from below, salted from above, and step function salinity gradients with depth ratio for various values of the thermal Marangoni number  $Ma_T = 5, Ma_T = 10$ , and  $Ma_T = 15$ . The other dimensionless parameters are fixed as  $Da = 0.03, M_{aT} = 5, M_{aS} = 5, R_I = 0.1, S_r = 0.5, R_{aS} = 100, \hat{\kappa}_T = 1.0$ , and  $\tau = 0.3$ . We observe that the increase in  $Ma_T$  increases  $Ra_C$  for all six salinity gradients. An increase in  $Ma_T$  increases the surface tension of the fluid, which declines the onset of convection. Hence, the increase in  $Ma_T$  stabilizes the onset of Rayleigh-Benard Marangoni convection.

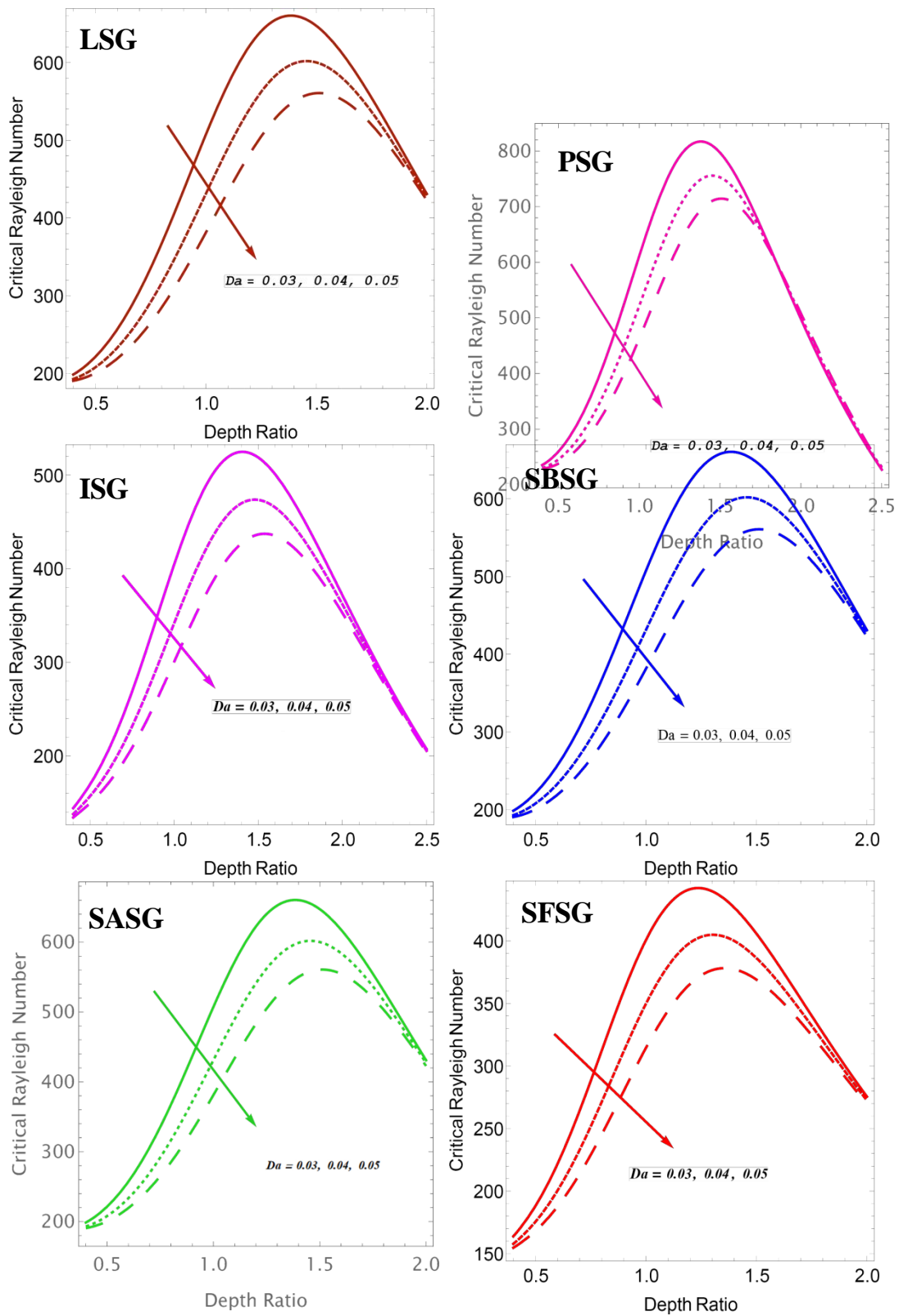


Figure 2: The effect of Darcy number ( $Da$ ) on critical Rayleigh number ( $R_{ac}$ )

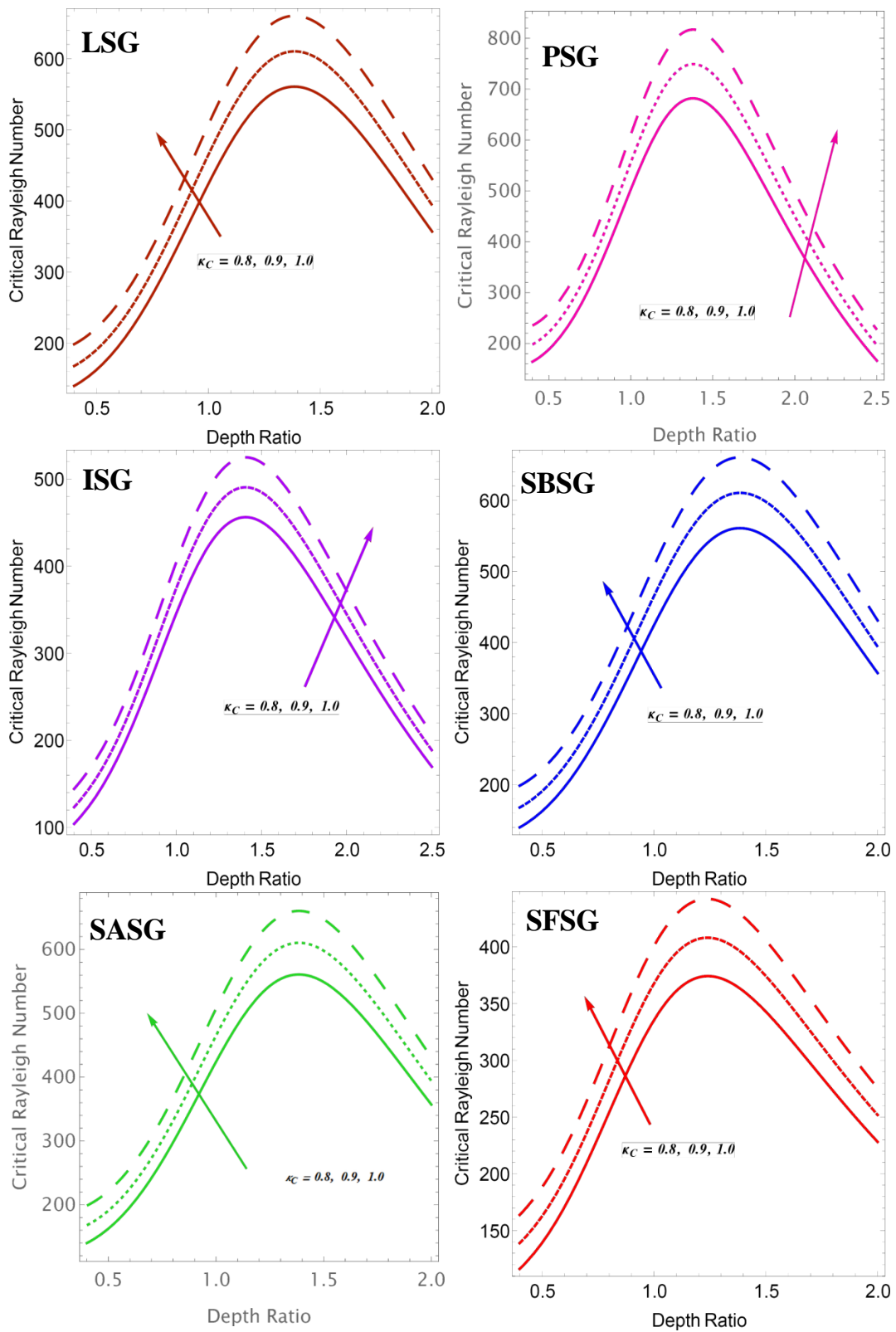


Figure 3: The effect of Solute diffusivity ( $\kappa_C$ ) on critical Rayleigh number ( $R_{ac}$ )

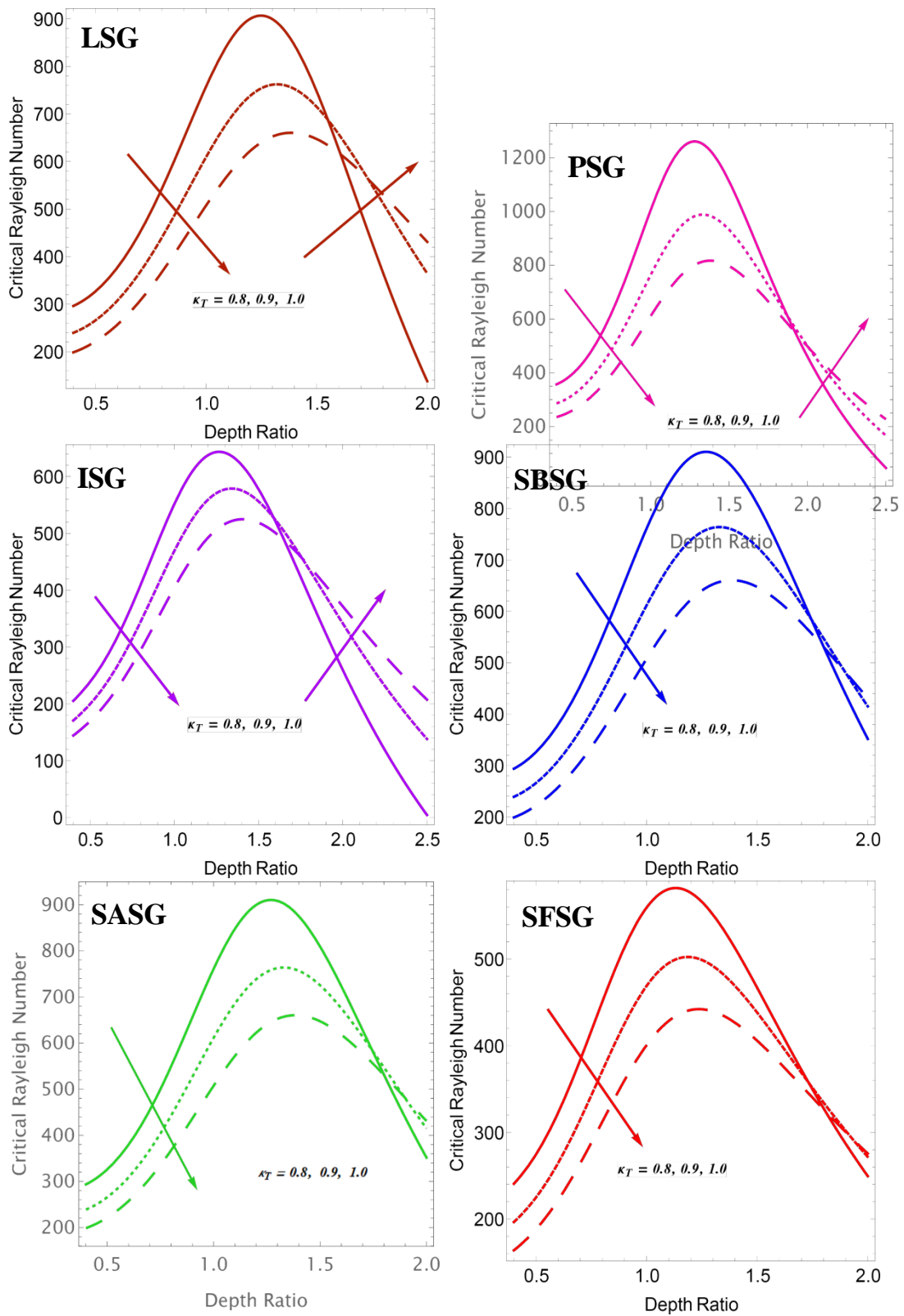


Figure 4: The effect of Thermal diffusivity ( $\kappa_T$ ) on critical Rayleigh number ( $R_{ac}$ )

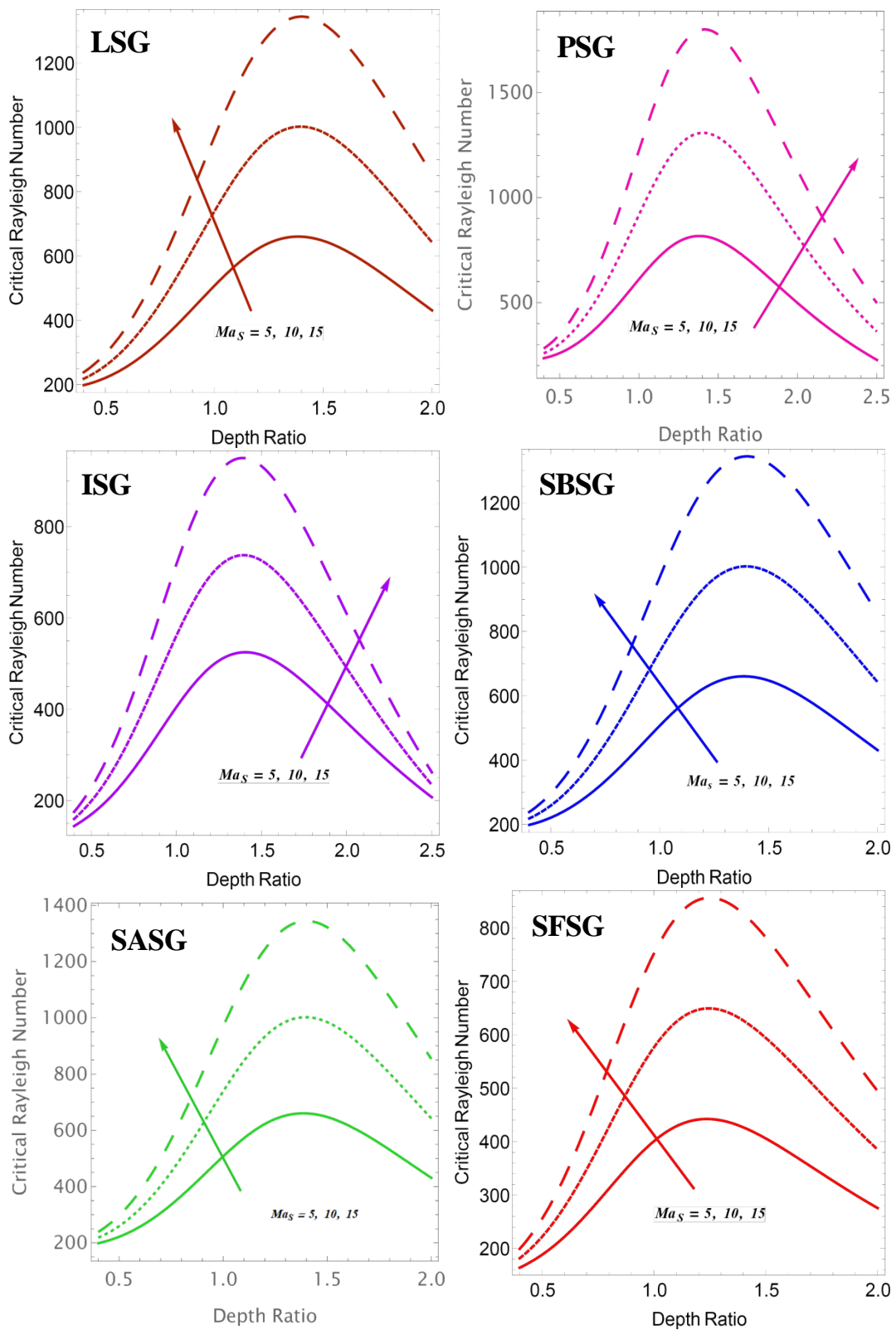


Figure 5: The effect of Solute marangoni number ( $Ma_S$ ) on critical Rayleigh number ( $Ra_c$ )

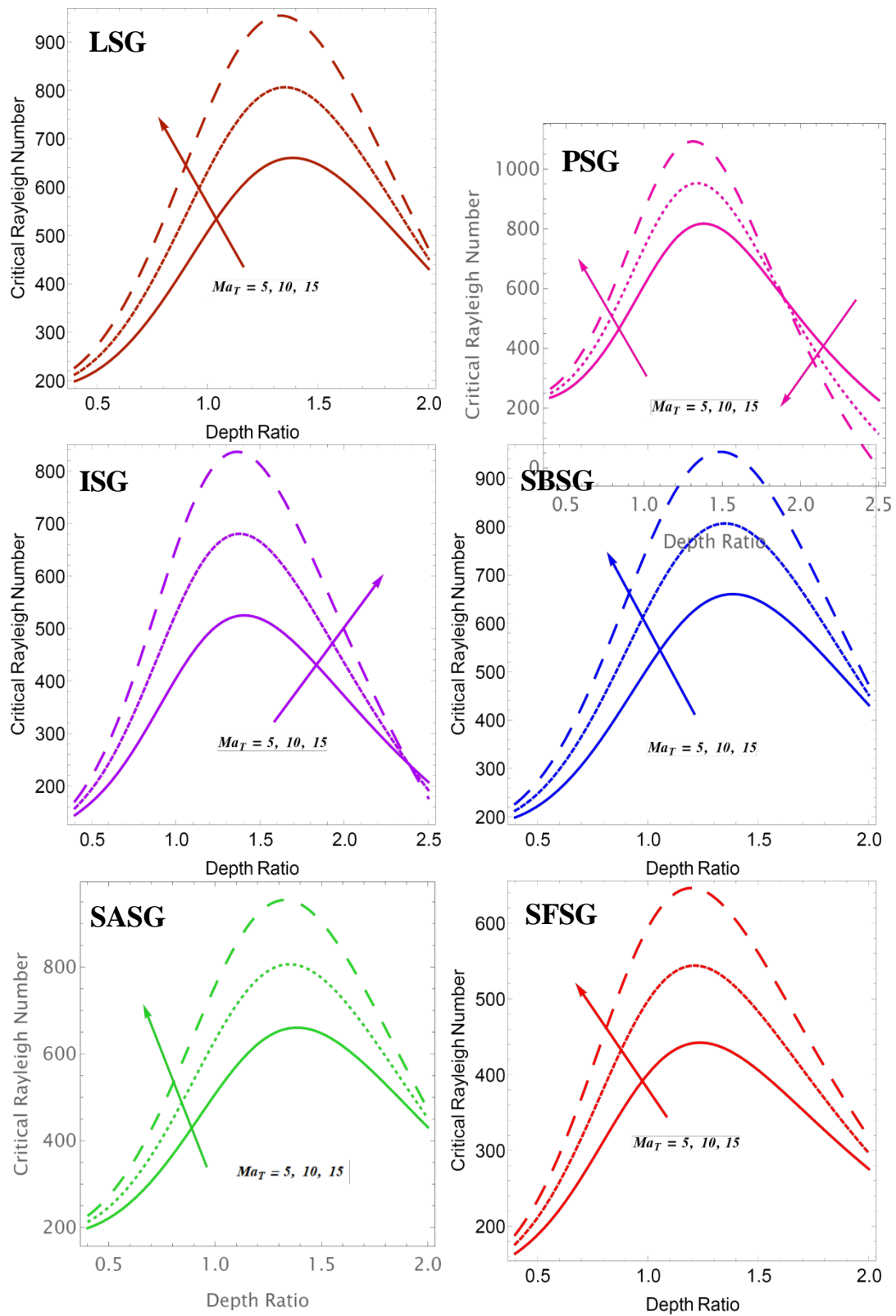


Figure 6: The effect of Thermal marangoni number ( $Ma_T$ ) on critical Rayleigh number ( $Rac$ )

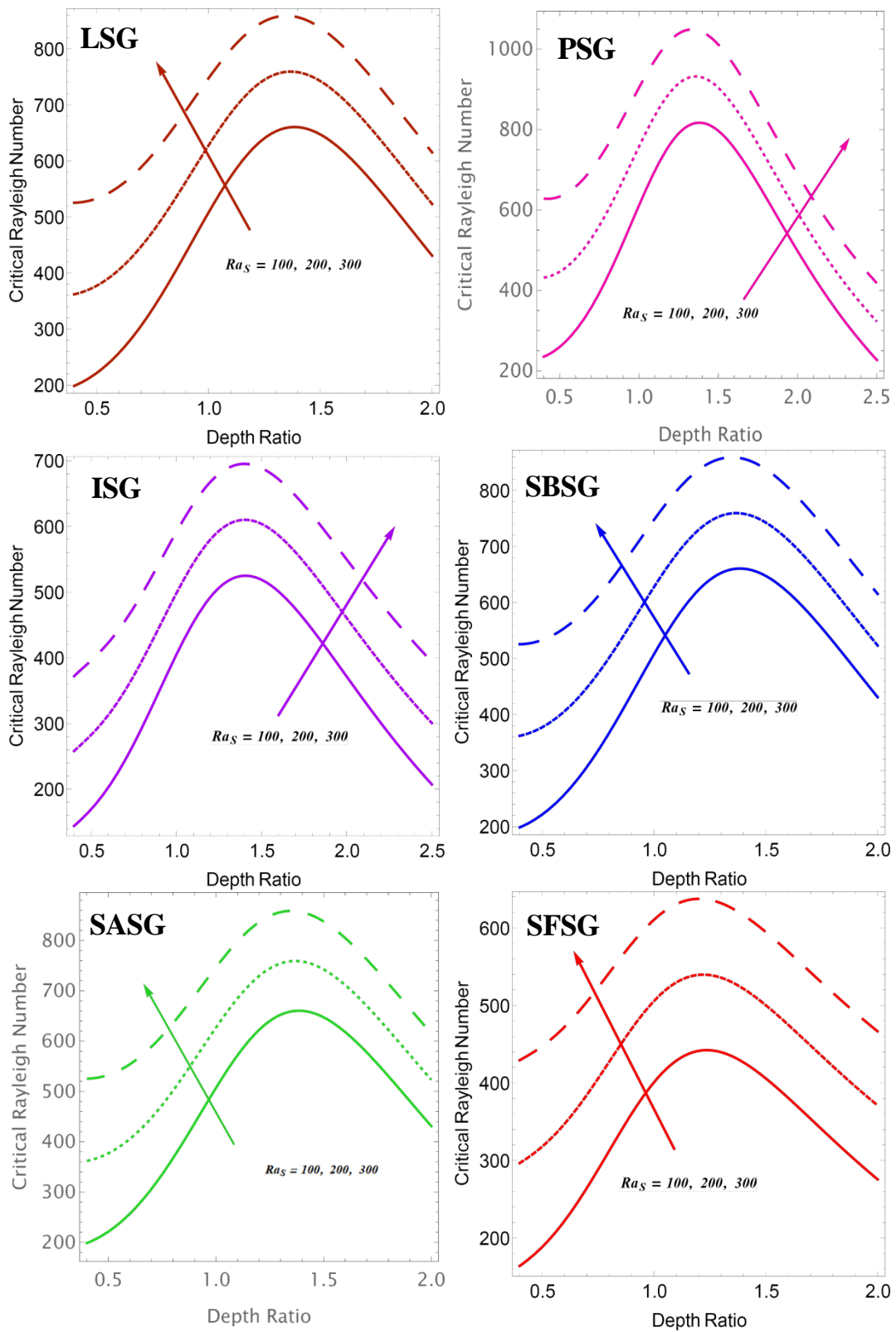


Figure 7: The effect of Solute Rayleigh number ( $Ra_S$ ) on critical Rayleigh number ( $Ra_c$ )

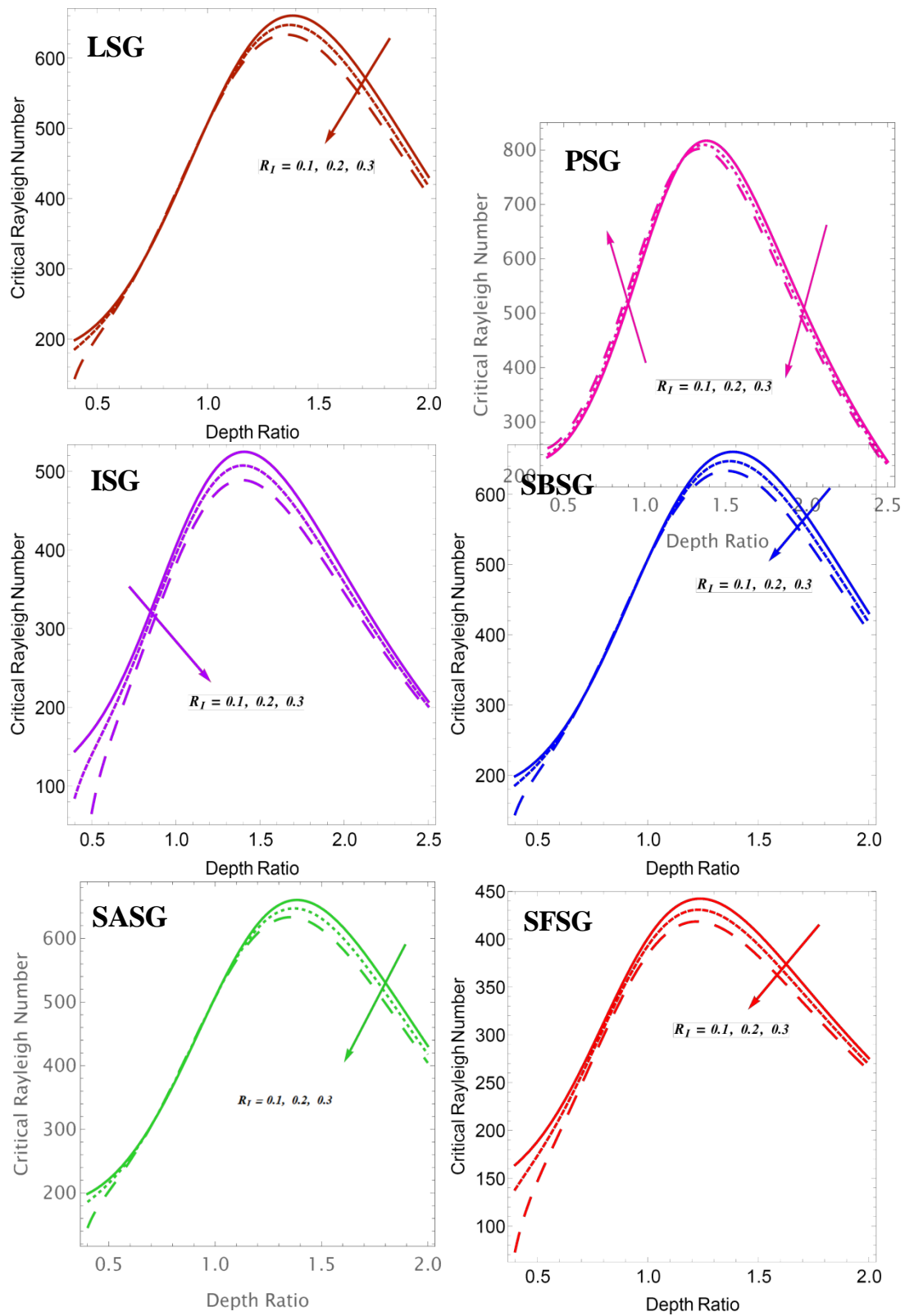


Figure 8: The effect of Internal Rayleigh number ( $R_I$ ) on critical Rayleigh number ( $R_{ac}$ )

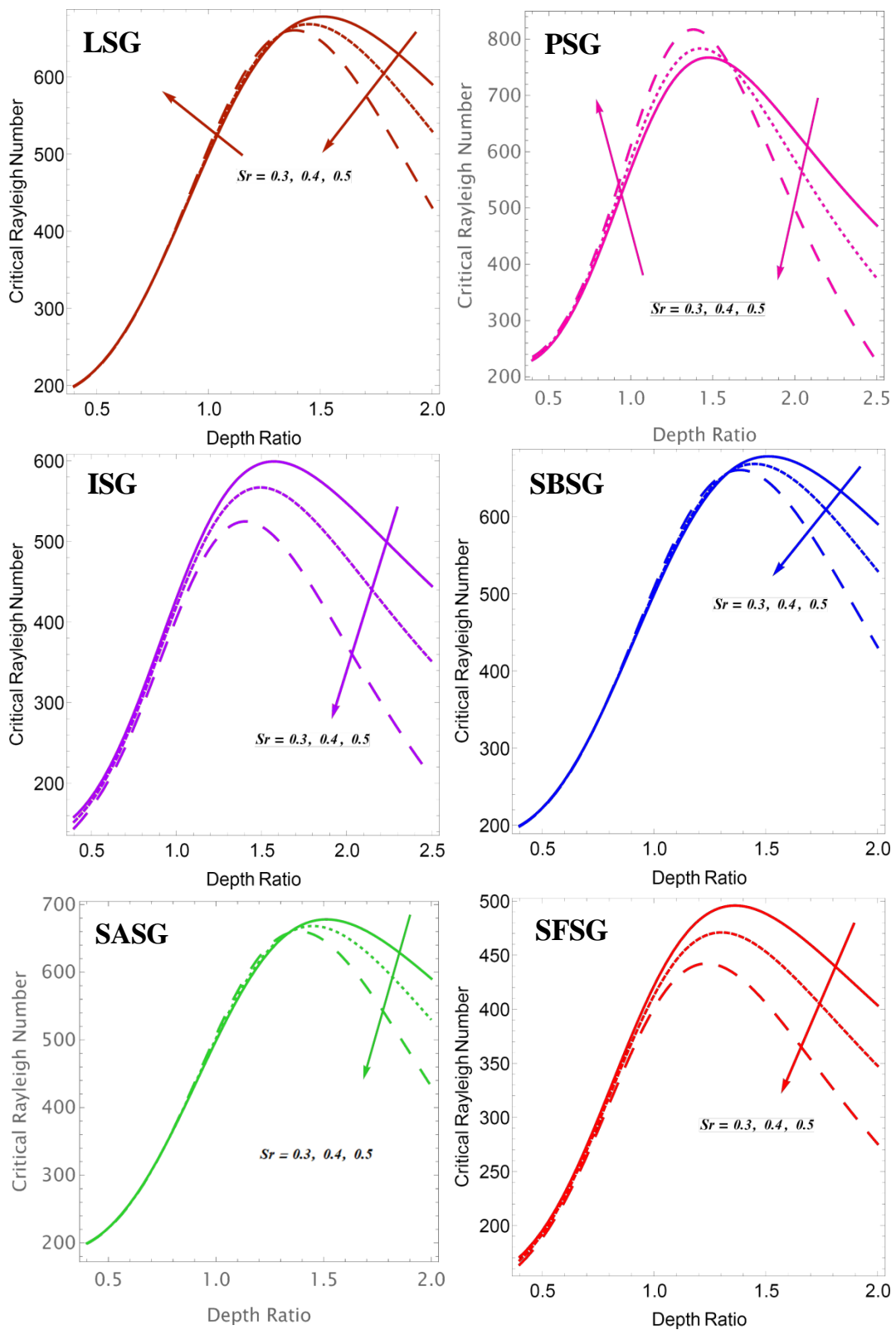


Figure 9: The effect of Soret number ( $Sr$ ) on critical Rayleigh number ( $Rac$ )

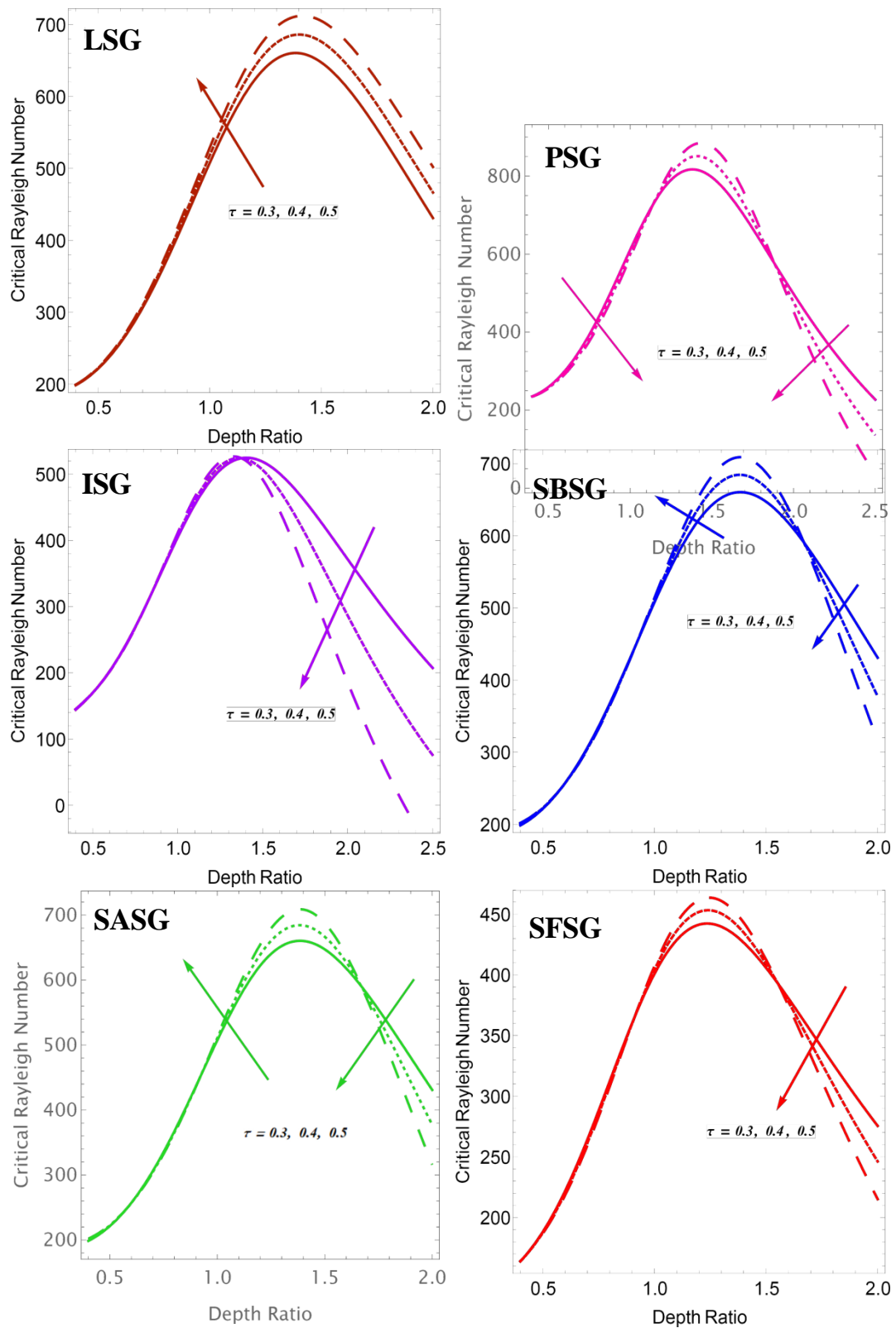


Figure 10: The effect of Diffusivity ratio ( $\tau$ ) on critical Rayleigh number ( $R_{ac}$ )

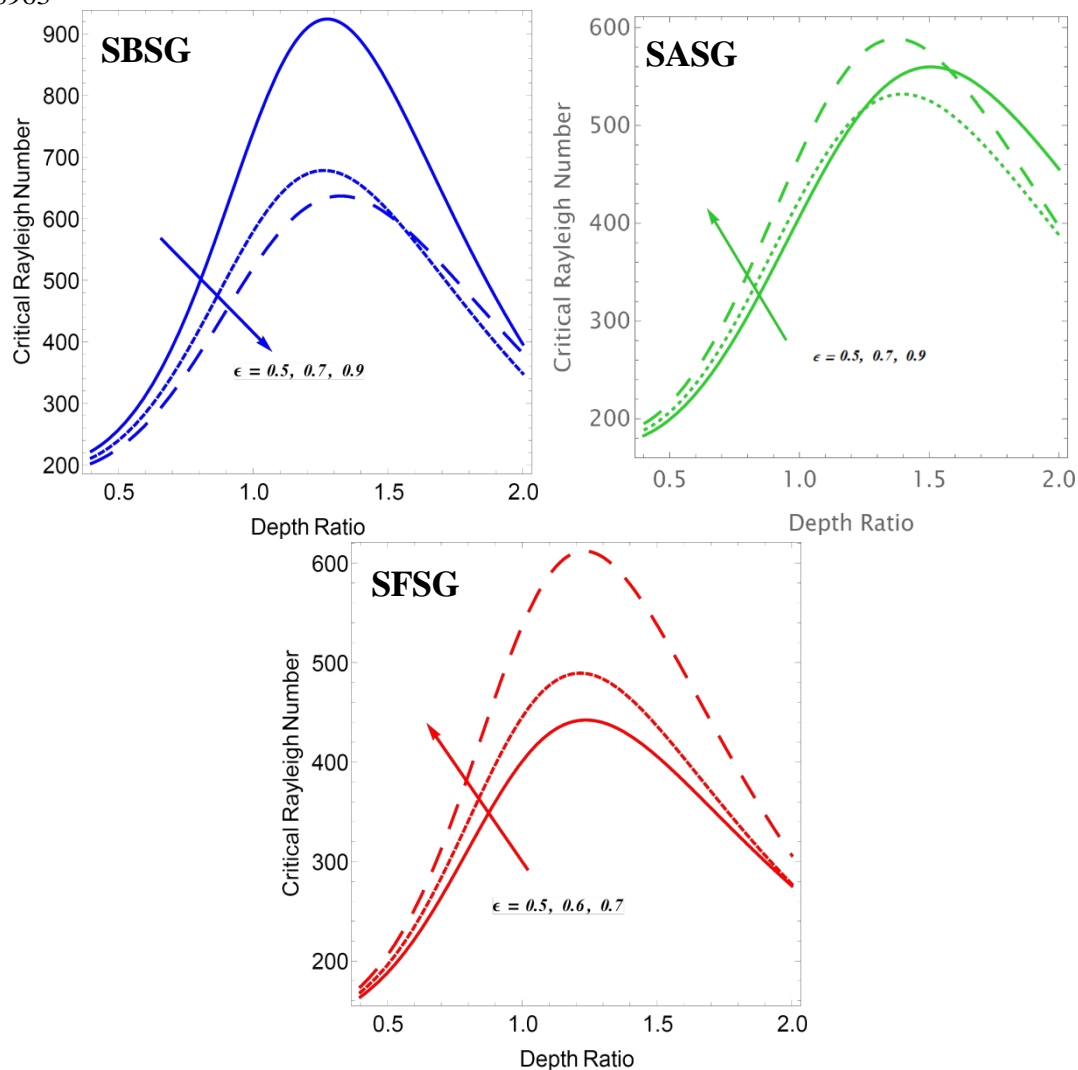


Figure 11: The effect of Thermal Depth ( $\epsilon$ ) on critical Rayleigh number ( $Ra_C$ )

**Figure (7)** depicts the distinction of critical Rayleigh numbers for linear, parabolic, and inverted parabolic salted from below, salted from above, and step function salinity gradients with depth ratio for various values of the Solute Rayleigh number  $Ra_s = 100$ ,  $Ra_s = 200$ , and  $Ra_s = 300$ . The other dimensionless parameters are fixed as  $Da = 0.03$ ,  $Ma_T = 5$ ,  $Ma_S = 5$ ,  $R_I = 0.1$ ,  $S_r = 0.5$ ,  $R_{as} = 100$ ,  $\hat{\kappa}_T = 1.0$ , and  $\tau = 0.3$ . We observe that the increase in  $Ra_s$  increases  $Ra_C$  for all six salinity gradients. An increase in  $Ra_s$  increases the concentration of the fluid, which declines the onset of convection. Hence, the increase in  $Ra_s$  stabilizes the onset of Rayleigh-Benard Marangoni convection. **Figure (8)** depicts the distinction of critical Rayleigh numbers for linear, parabolic, and inverted parabolic salted from below, salted from above, and step function salinity gradients with depth ratio for various values of the internal thermal Rayleigh number  $R_I = 0.1$ ,  $R_I = 0.2$ , and  $R_I = 0.3$ . The other dimensionless parameters are fixed as  $Da = 0.03$ ,  $Ma_T = 5$ ,  $Ma_S = 5$ ,  $R_I = 0.1$ ,  $S_r = 0.5$ ,  $R_{as} = 100$ ,  $\hat{\kappa}_T = 1.0$ , and  $\tau = 0.3$ . We observe that the increase

in  $R_I$  increases  $Ra_C$  for inverted parabolic salinity gradient and decreases for linear and parabolic salinity gradients. An increase in  $R_I$  increases the internal heat source of the fluid, which hastens the onset of convection. Hence, the increase in  $R_I$  destabilizes the onset of Rayleigh- Benard Marangoni convection. **Figure (9)** depicts the distinction of critical Rayleigh numbers for linear, parabolic, and inverted parabolic salted from below, salted from above, and step function salinity gradients with depth ratio for various values of the solet number  $S_r = 0.3$ ,  $S_r = 0.4$ , and  $S_r = 0.5$ . The other dimensionless parameters are fixed as  $D_a = 0.03$ ,  $M_{aT} = 5$ ,  $M_{aS} = 5$ ,  $R_I = 0.1$ ,  $S_r = 0.5$ ,  $R_{aS} = 100$ ,  $\hat{\kappa}_T = 1.0$ , and  $\tau = 0.3$ . We observe that the increase in  $S_r$  increases  $Ra_C$  for all salinity gradients. An increase in  $S_r$  increases thermal diffusivity in the system which hastens the onset of convection. Hence, the increase in  $S_r$  destabilizes the onset of Rayleigh-Benard Marangoni convection. **Figure (10)** depicts the distinction of critical Rayleigh numbers for linear, parabolic, and inverted parabolic salted from below, salted from above, and step function salinity gradients with depth ratio for various values of the solute to thermal diffusivity ratio  $\hat{\tau} = 0.3$ ,  $\hat{\tau} = 0.4$ , and  $\hat{\tau} = 0.5$ . The other dimensionless parameters are fixed as  $D_a = 0.03$ ,  $M_{aT} = 5$ ,  $M_{aS} = 5$ ,  $R_I = 0.1$ ,  $S_r = 0.5$ ,  $R_{aS} = 100$ ,  $\hat{\kappa}_T = 1.0$ , and  $\tau = 0.3$ . We observe that the increase in  $\tau$  increases  $Ra_C$  for linear and inverted parabolic salinity gradients and decreases for parabolic salinity gradient. An increase in  $\hat{\tau}$  increases solute diffusivity in the system which declines the onset of convection. Hence, the increase in  $\tau$  stabilizes the onset of Rayleigh-Benard Marangoni convection. **Figure (11)** depicts the distinction of critical Rayleigh numbers for salted from below, salted from above, and step function salinity gradients with depth ratio for various values of the thermal depth  $\epsilon = 0.5$ ,  $\epsilon = 0.7$ , and  $\epsilon = 0.9$ . The other dimensionless parameters are fixed as  $D_a = 0.03$ ,  $M_{aT} = 5$ ,  $M_{aS} = 5$ ,  $R_I = 0.1$ ,  $S_r = 0.5$ ,  $R_{aS} = 100$ ,  $\hat{\kappa}_T = 1.0$ , and  $\tau = 0.3$ . We observe that the increase in  $\epsilon$  increases  $Ra_C$  for salting from above and step function salinity gradients and decreases for salting from below salinity gradient. An increase in  $\epsilon$  increases solute diffusivity in the system which declines the onset of convection for salting from above and step function salinity gradients stabilizes the onset of Rayleigh- Benard Marangoni convection. Whereas, for salting from below salinity gradients the thermal diffusivity increases. Hence, destabilizes the onset of Rayleigh-Benard Marangoni convection.

## Conclusions

Double Diffusive Rayleigh-Barnard-Marangoni (DDRBM) convection in a composite layered system, incorporating the Soret effect, constant heat source and the effect of linear ( $Rc_1$ ), parabolic ( $Rc_2$ ), inverted parabolic ( $Rc_3$ ), salted from below ( $Rc_4$ ), salted from above ( $Rc_5$ ), and step function ( $Rc_6$ ) salinity gradients is analyzed and solved in closed form using the Regular Perturbation method. This study investigates the interplay between thermal and solutal buoyancy forces, surface tension gradients, and the Soret-driven mass diffusion on the stability and dynamics of the system.

The following conclusions are drawn:

1. Effect of increasing the values of solute diffusivity increases the critical Rayleigh number for all six salinity gradients. Consequently, it stabilizes the onset of double diffusive Rayleigh Benard Marangoni convection with constant heat source.
2. Effect of increasing the values of solute Rayleigh number increases the critical Rayleigh number for all six salinity gradients. Consequently, it stabilizes the onset of double diffusive Rayleigh Benard Marangoni convection with constant heat source.
3. Effect of increasing the values of ratio of solute to thermal diffusivity increases the critical Rayleigh number for all six salinity gradients. Consequently, it stabilizes the onset of double diffusive Rayleigh Benard Marangoni convection with constant heat source.
4. Effect of increasing the values of thermal Marangoni number increases the critical Rayleigh number for all six salinity gradients. Consequently, it stabilizes the onset of double diffusive Rayleigh Benard Marangoni convection with constant heat source.
5. Effect of increasing the values of solute Marangoni number increases the critical Rayleigh number for all six salinity gradients. Consequently, it stabilizes the onset of double diffusive Rayleigh Benard Marangoni convection with constant heat source.
6. Effect of increasing the values of Darcy number decreases critical Rayleigh number for all six salinity gradients. Consequently, it destabilizes the onset of double diffusive Rayleigh Benard Marangoni convection with constant heat source.
7. Effect of increasing the values of Soret number decreases critical Rayleigh number for all six salinity gradients. Consequently, it destabilizes the onset of double diffusive Rayleigh Benard Marangoni convection with constant heat source.
8. Effect of increasing the values of internal Rayleigh number decreases critical Rayleigh number for all six salinity gradients. Consequently, it destabilizes the onset of double diffusive Rayleigh Benard Marangoni convection with constant heat source.

9. Effect of increasing the values of thermal diffusivity ratio decreases critical Rayleigh number for all six salinity gradients. Consequently, it destabilizes the onset of double diffusive Rayleigh Benard Marangoni convection with constant heat source.
10. Upto depth ratio  $\hat{d} = 1.5$ , the critical Rayleigh number increases for all parameters beyond which critical Rayleigh number decreases for linear, parabolic, inverted parabolic salted from below, salted from above and step function salinity gradients.

## References

- 1] R. A. Pearson, "On convection cells induced by surface tension", 1958.
- 2] D. A. Nield, "Onset of convection in a Fluid Layer Overlying a Layer of porous Medium", *J Fluid Mech.* 81, 1977, 513-522
- 3] F. Chen and C. F. Chen, "Experimental investigation of convective stability in a superposed fluid and porous layer when heated from below", *J Fluid Mech.* vol. 207, pp. 311- 321, 1989.
- 4] A. Silberstein, C. Langlais, and E. Arquis, "Natural Convection in Light Fibrous Insulating Materials with Permeable Interfaces: Onset Criteria and Its Effect on the Thermal Performances of the Product", *Journal of Thermalinsulation*, vol. 14, pp. 22-42, July, 1990.
- 5] D. A. Nield, A. Bejan, *Convection in Porous Media*, Springer-Verlag: New York, 1992.
- 6] S. J. Kim and C. Y. Choi, "Convective heat transfer in porous and overlying fluid layers heated from below", *Int. J Heat Mass Transfer*, vol. 39, no. 2, pp. 319-329, 1996.
- 7] A. Bergeon, D. Henry, H. Benhadid, and L. S. Tuckerman, "Marangoni convection in binary mixtures with Soret effect", *J Fluid Mech.* val. 375, pp. 143-177, 1998.
- 8] M. Z. Saghir, M. Hennenberg, and M. R. Islam, "Double Diffusive and Marangoni Convection in a Multi-Cavity System", *Int. J. of Heat Mass Transfer*, vol. 41, no. 14, pp. 2157- 2174, 1998.
- 9] D. Schwabe, A. Cramer, J. Scheneider, S. Benz and J. Metzger, "Experiments on the multi-roll-structure of thermocapillary flow in side-heated thin liquid layers", *Adv. Space Res.* vol. 24, no. 10, pp. 1367-1373, 1999.
- 10] D. Schwabe, "The Benard-Marangoni-instability In small circular containers under microgravity: experimental results", *Adv. Space Res.* vol. 24, no. 10, pp. 1347-1356, 1999.
- 11] J. Tanny and B. Yakubov, "Experimental study of a double-diffusive two-layer system in a laterally heated enclosure", *Int. J of heat and mass transfer*, vol. 42, pp. 3619-3629, 1999.
- 12] A. Bahloul, R. Delahaya, P. Vasseur, and L. Robillard, "Effect of Surface Tension on Convection in a Binary Fluid Layer Under Zero Gravity Environment", *International Journal of Heat and Mass Transfer*, vol. 46, pp. 1759-1771, 2003.
- 13] C. G. Jiang, M. Z. Saghir, M. Kawaji, and K. Ghorayeb, "Two-dimensional numerical simulation of thermogravitational convection in a vertical porous column filled with a binary fluid mixture", *Int. J of thermal Science*, val. 43, pp. 1057-1065, 2004.
- 14] Adrian Postelnicu, "Influence of a magnetic field on heat and mass transfer by natural convection from vertical surfaces in porous media considering Soret and Dufour effects", *International Journal of Heat and Mass Transfer*, Volume 47, Issues 6-7, Pages 1467-1472, 2004.

- 15] R. Kozak, M. Z. Saghir, and A. Viviani, "Marangoni convection in a liquid layer overlying a porous layer with evaporation at the free surface", *Acta Astronautica*, vol. 55, pp. 189-197, 2004.
- 16] M. Z. Saghir, P. Mahendran and M. Hennenberg, "Marangoni and Gravity Driven Convection in a Liquid Layer Overlying a Porous Layer: Lateral and Bottom Heating Conditions", *Energy Sources*, vol. 27, pp. 151-171, 2005.
- 17] J. K. Platten, "The Soret effect: review of recent experimental results", *J of Applied Mechanics*, val. 73, pp. 5-15, 2006.
- 18] D. V. Alexandrov, and D. L. Aseev, "Directional solidification with a two-phase zone: thermodiffusion and temperature-dependent diffusivity", *Computational Materials Science*, val. 37, pp. 1-6, 2006.
- 19] L. Ming-chun, T. Yan-wen, "Soret and Dufour effects in strongly endothermic chemical reaction system of porous media", *Trans nonferrous Mot. Soc.* vol. 16, pp. 1200-1204, 2006.
- 20] I. S. Shivakumara, S.P. Suma, K. B. Chavaraddi, "Onset of surface-tension-driven convection in superposed layers of fluid and saturated porous medium", *Arch. Mech.*, vol. 58, 2, pp. 71-92, Warszawa 2006.
- 21] A. Mansour, A. Amahmid, and M. Hasnaoui, "Soret effect of thermosolutal convection developed in a horizontal shallow porous layer salted from below and subject to cross fluxes of heat", *Int. J of Heat and Fluid Flow*, val. 29, pp. 306-314, 2008.
- 22] Benoit T., Eric C., Frederic D., Claudine D., Beatrice G., "Transient Rayleigh-Bénard-Marangoni solutal convection", *Physics of Fluids*, volume 24, issue 7, July 2012.
- 23] Balla, C. S., and Naikoti, K. , "Soret and Dufour effects on free convective heat and solute transfer in fluid saturated inclined porous cavity", *Engineering Science and Technology an International Journal*, 18(4)pp., 543- 554, 2015.
- 24] Sumithra R., Komala B., and Manjunatha, N. , "Darcy-Benard double diffusive Marangoni convection with Soret effect in a composite layer system", *Malaya Journal of Matematik (MJM)*, 8(4), pp. 1473-1479, 2020.
- 25] Sumithra R., Komala B., and Manjunatha, N. , "The onset of Darcy-Brinkman-convection in a composite system with thermal diffusion", *Heat Transfer*, 51(1), pp. 604-620, 2022.
- 26] Izzati Khalidah ,Nor Fadzillah Mohd Mokhtar, Zarina Bibi Ibrahim, "Control Effect on Rayleigh-Benard Convection in Rotating Nanofluids Layer with Double-Diffusive Coefficients", *CFD letters*, vol 14 pp.3, 2022.
- 27] Sumithra R., Komala B., "Onset of triple diffusive thermosolutal convection in a composite system", *Heat Transfer*, pp.2974-2994, 20



